Potential benefits of solar reflective car shells: cooler cabins, fuel savings and emission reductions

Ronnen Levinson, Heng Pan, George Ban-Weiss, Pablo Rosado,
Riccardo Paolini[1] and Hashem Akbari[2]

Lawrence Berkeley National Laboratory
One Cyclotron Road
Berkeley, CA 94720

source text for *Applied Energy*, 2011-05-19

Abstract

Vehicle thermal loads and air conditioning ancillary loads are strongly influenced by the absorption of solar energy. The adoption of solar reflective coatings for opaque surfaces of the vehicle shell can decrease the "soak" temperature of the air in the cabin of a vehicle parked in the sun, potentially reducing the vehicle's ancillary load and improving its fuel economy by permitting the use of a smaller air conditioner. An experimental comparison of otherwise identical black and silver compact sedans indicated that increasing the solar reflectance (ρ) of the car's shell by about 0.5 lowered the soak temperature of breath-level air by about 5-6°C. Thermal analysis predicts that the air conditioning capacity required to cool the cabin air in the silver car to 25°C within 30 minutes is 13% less than that required in the black car. Assuming that potential reductions in AC capacity and engine ancillary load scale linearly with increase in shell solar reflectance, ADVISOR simulations of the SC03 driving cycle indicate that substituting a typical cool-colored shell ($\rho = 0.35$) for a black shell ($\rho = 0.05$) would reduce fuel consumption by 0.12 L per 100 km (1.1%), increasing fuel economy by 0.10 km L^{-1} [0.24 mpg] (1.1%). It would also decrease carbon dioxide (CO_2) emissions by 2.7 g km^{-1} (1.1%), nitrogen oxide (NO_x) emissions by 5.4 mg km^{-1} (0.44%), carbon monoxide (CO) emissions by 17 mg km^{-1} (0.43%), and hydrocarbon (HC) emissions by 4.1 mg km^{-1} (0.37%). Selecting a typical white or silver shell ($\rho = 0.60$) instead of a black shell would lower fuel consumption by 0.21 L per 100 km (1.9%), raising fuel economy by 0.19 km L^{-1} [0.44 mpg] (2.0%). It would also decrease CO_2 emissions by 4.9 g km^{-1} (1.9%), NO_x emissions by 9.9 mg km^{-1} (0.80%), CO emissions by 31 mg km^{-1} (0.79%), and HC emissions by 7.4 mg km^{-1} (0.67%). Our simulations may underestimate emission reductions because emissions in standardized driving cycles are typically lower than those in real-world driving.

---

[1] Currently at Department of Building Environment Science & Technology, Politecnico di Milano, Milano, Italy

[2] Currently at Department of Building, Civil, and Environmental Engineering, Concordia University, Montreal, Canada

Disclaimer

This document was prepared as an account of work sponsored by the United States Government. While this document is believed to contain correct information, neither the United States Government nor any agency thereof, nor the Regents of the University of California, nor any of their employees, makes any warranty, express or implied, or assumes any legal responsibility for the accuracy, completeness, or usefulness of any information, apparatus, product, or process disclosed, or represents that its use would not infringe privately owned rights. Reference herein to any specific commercial product, process, or service by its trade name, trademark, manufacturer, or otherwise, does not necessarily constitute or imply its endorsement, recommendation, or favoring by the United States Government or any agency thereof, or the Regents of the University of California. The views and opinions of authors expressed herein do not necessarily state or reflect those of the United States Government or any agency thereof or the Regents of the University of California.

Introduction

Over 95% of the cars and small trucks sold in California have air conditioning (Daly 2006; EPA 2009). Use of air conditioning (AC) in cars has been estimated to increase carbon monoxide (CO) emissions by 0.99 g km^{-1} (71%), increase nitrogen oxide (NO_x) emissions by 0.12 g km^{-1} (81%), and reduce fuel economy by 2.0 km L^{-1} [4.6 mpg] (22%) (Bevilacqua 1999). Air conditioning is the major ancillary load for a light-duty vehicle. The AC is sized to cool the cabin air from its "hot soak" condition (i.e., vehicle parked in the sun, facing the equator, on a summer afternoon) to a comfortable quasi-steady temperature, such as 25°C. Reducing the peak cooling load lowers the required cooling capacity, reducing ancillary load, improving fuel economy, and decreasing tailpipe emissions.

The current study focuses on the decrease in soak temperature, reduction in AC capacity, and improvement in fuel economy attainable through the use of solar reflective shells. Here "shell" refers to the opaque elements of the car's envelope, such as its roof and doors. First, we experimentally characterize component temperatures and cooling demands in a pair of otherwise identical dark and light colored vehicles, the former with low solar reflectance and the latter with high solar reflectance. Second, we employ a thermal model to predict the AC capacity required to cool each vehicle to a comfortable final cabin air temperature. Third, we use the AVL ADVISOR vehicle simulation tool to estimate the dependence on ancillary load of the fuel consumption and pollutant emissions of a comparable prototype vehicle in various standard drive cycles. Finally, we calculate the fuel savings and emission reductions attainable by using a cool shell to reduce ancillary load.

Literature review

Extensive research over the past two decades has focused on reducing air conditioner ancillary loads. Most studies consider cabin air temperature, AC cooling load, and/or occupant comfort.

Technology performance

Technologies to reduce AC load include solar reflective glazing, solar reflective shells, ventilation, insulation and window shading (Rugh et al. 2001; Turler et al. 2003; Hoke and Greiner 2005; Rugh and Farrington 2008; Han and Chen 2009). Past research has identified the use of solar reflective glazing as an especially effective strategy for reducing cooling loads since sunlight transmitted through glazing accounts for 70% of cabin heat gain in hot soak conditions (Sullivan and Selkowitz 1990). For example, Rugh et al. (2001) measured that solar reflective glazing in a Ford Explorer decreased cabin air ("breath") temperature by 2.7°C, lowered instrument panel temperatures by 7.6°C, and reduced windshield temperatures by 10.5°C. They also reported that this decrease in cabin air soak temperature would permit an 11% reduction in

AC compressor power. More generally, they estimated that AC compressor power could be decreased by about 4.1% per 1°C reduction in cabin soak temperature.

Akabane et al. (1989) experimentally determined that in a vehicle traveling 40 km/h (25 mph) on a hot day (outdoor air temperature 38°C, horizontal solar irradiance 0.81 kW/m^2), about 42% of the vehicle heat load resulted from transmission through the glazing, with about 48% from conduction through the shell and about 10% from engine heat and air leaks. We note that load fractions may vary with window opacity and with the ratio of window area to shell area.

Rugh and Farrington (2008) found that ventilation and window shading during soak can be effective in reducing AC loads. They concluded that natural ventilation (achieved using appropriately placed inlets to allow for natural convection) can be almost as effective as forced ventilation.

Solar reflective shells have also been reported to reduce soak temperatures. Hoke and Greiner (2005) used the RadTherm and UH3D modeling tools to simulate soak conditions for a sport utility vehicle (SUV) parked on a hot summer day in Phoenix, AZ. They concluded that each 0.1 increase in the solar reflectance ρ of the shell reduces the cabin air soak temperature by about 1°C. For example, cabin air soak temperature in a vehicle with a white shell (ρ=0.50) was predicted to be 4.6°C lower than that in a comparable vehicle with a black shell (ρ=0.05). Rugh and Farrington (2008) measured for several vehicles the reduction in cabin air (breath) soak temperature versus increase in shell solar reflectance. Increasing the shell solar reflectance of a Ford Explorer mid-size SUV by 0.44 lowered cabin air soak temperature by 2.1°C (0.47°C reduction per 0.1 gain in shell solar reflectance), while increasing that of a Lincoln Navigator full-size SUV by 0.45 lowered cabin air soak temperature by 5.6°C (1.2°C reduction per 0.1 gain in shell solar reflectance). Increasing the solar reflectance of only the roof of a Cadillac STS full-size sedan by 0.76 lowered cabin air temperature by 1.2°C (0.15°C reduction per 0.1 gain in roof solar reflectance).

A 3-D computational fluid dynamics (CFD) simulation by Han and Chen (2009) estimated that increasing body insulation reduces steady state thermal load, but raises air cabin temperature during soaking and cooling.

Modeling tools

Simulations of thermal load and thermal comfort in vehicles typically use either lumped-parameter models (Heydari and Jani 2001; Turler et al. 2003; Huang et al. 2007; Junior et al. 2009) or transient CFD models (Henry et al. 2001; Taxis-Reischl et al. 2001; Wolfahrt et al. 2005; Zhang et al. 2009a,b). A study by the National Renewable Energy Laboratory (NREL) concluded that transient CFD tools are best suited for this task (Cullimore and Hendricks 2001).

Bharatan et al. (2007) provide a definitive overview of the models that have been adopted or developed by NREL to simulate environmental loads, thermal comfort, and AC fuel use. We summarize some findings below.

Environmental forcing. The GUI-driven MATLAB application Vehicle Solar Load Estimator (VSOLE), developed by NREL (Rugh 2002), calculates the solar radiation transmitted, absorbed, and reflected by glazing as a function of glazing properties and location, vehicle geometry, vehicle orientation, time, and radiation source.

Thermal modeling. The commercial CFD tool RadTherm can be used to simulate solar heat load, interior and exterior convection, and conduction through the envelope, while the commercial CFD tool Fluent can be used to simulate convective heat transfer and fluid flow in the cabin.

AC performance. An NREL model uses transient analysis to optimize vehicle AC performance (Hendricks 2001a).

Fuel economy. The AVL ADVISOR vehicle simulator originally developed by National Renewable Energy Laboratory (NREL) (Wipke et al. 1999a,b) can simulate the effect of vehicle ancillary load on fuel consumption and pollutant emissions.

Thermal comfort. NREL has applied two models from the University of California at Berkeley—the Human Thermal Physiological Model and the Human Thermal Comfort Empirical Model—to evaluate thermal comfort in vehicles.

Theory

Cabin air temperature model

The cabin air heating rate, or rate at which the internal energy of the cabin air $U(t)$ increases with time t, is

$$\frac{dU}{dt} = m_{\mathrm{a}}\, c_{\mathrm{v}}\, \frac{dT_{\mathrm{a}}}{dt}, \tag{1}$$

where m_{a} is the cabin air mass, c_{v} is the specific heat of air at constant volume, and $T_{\mathrm{a}}(t)$ is the cabin air temperature. The cabin air is assumed to be transparent to both sunlight and thermal radiation, but exchanges heat with the air conditioner and the cabin surface. If the air is well mixed, a simple model for the variation of cabin air temperature with time is

$$\frac{dT_{\mathrm{a}}}{dt} = \alpha\left[T_{\mathrm{v}}(t) - T_{\mathrm{a}}(t)\right] + \beta\left[T_{\mathrm{s}}(t) - T_{\mathrm{a}}(t)\right], \tag{2}$$

where $T_{\mathrm{v}}(t)$ is the temperature of the air flowing into the cabin from the AC vent, $T_{\mathrm{s}}(t)$ is the mean temperature of the cabin's surface, and α and β are fitted constants.

As the cabin air is mechanically cooled, it may reach a quasi-steady state in which $T_{\mathrm{a}}(t)$ asymptotically approaches a final value. In this condition, denoted by the superscript *, $(dT_{\mathrm{a}}/dt)^* \approx 0$ and thus

$$T_{\mathrm{a}}^* \approx T_{\mathrm{v}}^* + \frac{\beta}{\alpha}(T_{\mathrm{s}} - T_{\mathrm{a}})^* . \tag{3}$$

We may need to lower the vent air temperature if the final cabin air temperature T_{a}^* exceeds some design target $T_{\mathrm{a}}'^*$, such as 25°C. If the difference between the cabin surface temperature and the cabin air temperature $(T_{\mathrm{s}} - T_{\mathrm{a}})$ is insensitive to the vent air temperature T_{v}, then

$$\frac{dT_{\mathrm{a}}^*}{dT_{\mathrm{v}}^*} \approx 1 . \tag{4}$$

That is, reducing T_{v}^* by ΔT will lower T_{a}^* by approximately ΔT. Resizing the AC to yield a new vent air temperature $T_{\mathrm{v}}'(t) \equiv T_{\mathrm{v}}(t) - \Delta T$ results in a new cabin air temperature $T_{\mathrm{a}}'(t)$ that can be computed by numerically integrating

$$\frac{dT_{\mathrm{a}}'}{dt} = \alpha\left[T_{\mathrm{v}}'(t) - T_{\mathrm{a}}'(t)\right] + \beta\left[T_{\mathrm{s}}(t) - T_{\mathrm{a}}(t)\right] \tag{5}$$

subject to the initial condition $T_{\mathrm{a}}'(0) = T_{\mathrm{a}}(0)$. Note that the second term on the right hand side of Eq. (5) is the same as that in Eq. (2) because we've assumed that $T_{\mathrm{s}}'(t) - T_{\mathrm{a}}'(t) = T_{\mathrm{s}}(t) - T_{\mathrm{a}}(t)$.

AC capacity model

In recirculation mode, the rates at which the original and resized air conditioners remove heat from the cabin air are

$$q_{\mathrm{AC}}(t) = \dot{m}\, c_{\mathrm{p}}\left[T_{\mathrm{a}}(t) - T_{\mathrm{v}}(t)\right] \tag{6}$$

and

$$q_{\mathrm{AC}}'(t) = \dot{m}\, c_{\mathrm{p}}\left[T_{\mathrm{a}}'(t) - T_{\mathrm{v}}'(t)\right], \tag{7}$$

respectively, where $\dot{m}$ is the AC air mass flow rate and c_{p} is the specific heat of air at constant pressure. To meet peak cooling load, the capacity of the resized AC must be at least

$$Q \equiv \max\left[q'_{\mathrm{AC}}(t)\right] = \dot{m}\, c_{\mathrm{p}} \max\left[T'_{\mathrm{a}}(t) - T'_{\mathrm{v}}(t)\right]. \tag{8}$$

Fuel saving and emission reduction model

Consider two vehicles that differ only in shell solar reflectance ρ and required AC capacity Q. The reduction in AC capacity attainable by substituting the high-reflectance shell (subscript "H") for the low-reflectance shell (subscript "L") is

$$\Delta Q_{\mathrm{H}} \equiv Q_L - Q_{\mathrm{H}} \tag{9}$$

and the reduction in vehicle ancillary power load P is

$$\Delta P_{\mathrm{H}} = \Delta Q_{\mathrm{H}} / COP \tag{10}$$

where COP is coefficient of performance of the AC system.

Let F denote fuel consumption rate (volume of fuel per unit distance traveled) and E represent pollutant emission rate (mass of pollutant per unit distance traveled). If reductions in F and E are each linearly proportional to reduction in P, then

$$\Delta F_{\mathrm{H}} = \gamma_{\mathrm{F}}\, \Delta Q_{\mathrm{H}} / COP \tag{11}$$

and

$$\Delta E_{\mathrm{H}} = \gamma_{\mathrm{E}}\, \Delta Q_{\mathrm{H}} / COP \tag{12}$$

where $\gamma_{\mathrm{F}} \equiv dF/dP$ and $\gamma_{\mathrm{E}} = dE/dP$ are constant coefficients.

(We will show that for the drive cycles simulated in this study, γ_{F} and γ_{E} are indeed nearly constant within the ancillary power load ranges considered. However, past studies have raised doubt about the degree to which standardized driving cycles represent vehicle emissions from real-world driving (Samuel et al. 2002). Specifically, a disproportionate fraction of emissions occur from “off-cycle” driving characterized by high speed and/or acceleration. Bevilacqua (1999) has shown that NO_x and CO emissions are almost doubled with the operation of AC. Here the linearity assumption offers a very conservative estimate of pollutant reductions.)

Finally, consider a cool colored vehicle (subscript "C") that differs from the first two vehicles only in shell solar reflectance and required AC capacity. Since DOE-2 simulations indicate that reduction in a building’s annual peak demand for cooling power is linearly proportional to gain in roof solar reflectance (Konopacki et al. 1997), we assume that reduction in required AC capacity scales with increase in shell solar reflectance, such that

$$\Delta Q_{\mathrm{C}} \equiv Q_L - Q_{\mathrm{C}} = \frac{\rho_{\mathrm{C}} - \rho_{\mathrm{L}}}{\rho_{\mathrm{H}} - \rho_{\mathrm{L}}} \times \Delta Q_{\mathrm{H}}. \tag{13}$$

It then follows that the rates of fuel savings and emission reduction attainable by substituting the cool colored shell for the low-reflectance shell are

$$\Delta F_{\mathrm{C}} = \gamma_{\mathrm{F}}\, \Delta Q_{\mathrm{C}} / COP \tag{14}$$

and

$$\Delta E_{\mathrm{C}} = \gamma_{\mathrm{E}}\, \Delta Q_{\mathrm{C}} / COP \tag{15}$$

respectively.

Experiment (thermal study)

Overview

A pair of otherwise identical light duty vehicles, one with a black shell and the other with a silver shell, were instrumented with surface and air temperature sensors. AC performance was calibrated with an indoor heating and cooling trial. The vehicles were then parked outdoors on a sunny summer day and subjected to a series of five soaking and cooling trials.

Vehicles

Two 2009 Honda Civic 4DR GX compact sedans, one black and one silver, were loaned by California's Department of General Services (Figure 1). Apart from shell color, the vehicles were essentially identical, with only minor differences in odometer distance and AC line pressures (Table 1).

The air mass one global horizontal solar reflectance (Levinson et al. 2010a,b) of each exterior surface (roof) and interior surface (ceiling, dashboard, windshield, seat and door) was measured with a solar spectrum reflectometer (Devices & Services SSR-ER, version 6; Dallas, TX). The hemispherical thermal emittance of each roof and windshield was measured with an emissometer (Devices & Services AE1; Dallas, TX). The solar reflectances of the black and silver roofs were 0.05 and 0.58, respectively, while their thermal emittances were 0.83 and 0.79 (Table 2).

Instrumentation

The roof, ceiling, dashboard, windshield, seat, door, vent air and cabin air temperatures in each car were measured with thermistors (Omega SA1-TH-44006-40-T [surfaces], Omega SA1-TH-44006-120-T [air]; Stamford, CT) and recorded at 1 Hz with a portable data logger (Omega OM-DAQPRO-5300; Stamford, CT). The vent air thermistor was suspended in front of a central HVAC outlet, while the cabin air thermistor was suspended at breath level midway between the front seat headrests. Top and side views of the eight temperature measurement points in each vehicle are shown in Figure 2.

Each vent air and cabin air thermistor was wrapped in aluminum foil (low solar absorptance; low thermal emittance) to minimize both solar absorptance and radiative coupling to the cabin.[3] Interior surface thermistors (ceiling, dashboard, windshield, seat, and door) were wrapped in foil and secured with clear adhesive tape. Clear tape over foil yields high solar reflectance and high thermal emittance, minimizing solar absorptance while retaining radiative coupling to the cabin. Roof thermistors were affixed with reflectance-matched opaque adhesive tape. Black tape of solar reflectance 0.05 was used on the black roof (ρ =0.05), and a light-colored tape of solar reflectance 0.62 was used on the silver roof (ρ =0.58).

A weather station (Davis Instruments VantagePro2; Hayward, CA) mounted between the vehicles at a height of 2 m recorded 1 min averages of outside air temperature, relative humidity, global horizontal solar irradiance, and wind speed (Figure 1). Solar irradiance was also measured with a first-class pyranometer (Eppley Laboratory Precision Spectral Pyranometer; Newport, RI) to check the solar irradiance reported by the weather station's silicon radiometer. The first class pyranometer shared a datalogger channel with the black car's vent air thermistor. During daytime trials, the shared channel recorded vent air temperature while the vehicle was being cooled, and solar irradiance at other times.

AC calibration (16 July 2010)

On the evening of 16 July 2010, each vehicle was parked under a carport to shield it from sunlight. All windows were closed. At 18:38 LST, maximum heating (highest HVAC temperature setting, top fan speed, recirculation mode) was used to raise the cabin air temperature in each vehicle to about 60°C in 16 min. Each cabin's air temperature was then reduced to about 20°C after 20 min of maximum cooling (lowest HVAC temperature setting, top fan speed, recirculation mode). The cabin air and vent air temperatures during the cooling cycle in the black car were compared to those in the silver car to verify that the AC systems performed similarly.

Soaking and cooling (17 July 2010)

At 08:00 LST on the following day (17 July 2010), the vehicles were removed from the carport and parked outdoors, side by side, facing due south (Figure 1). All windows were closed.

[3] Increasing the thermal emittance of the sensor by replacing the foil with white paint (low solar absorptance, high thermal emittance) would tend to increase, rather than decrease, the apparent cabin air temperature by radiatively coupling the sensor to warm cabin surfaces. To illustrate, we note that the windshield in the black car has low solar absorptance and high thermal emittance (as would a white-coated sensor), but runs about 4°C warmer than the cabin air during the soak and about 13°C warmer than the cabin air during cooldown. These elevated windshield temperatures result from radiative coupling to the hot dashboard and ceiling.

The weather was warm and sunny, with the outside air temperature rising steadily from 21°C at 08:00 LST to 38°C at 16:00 LST. Global horizontal solar irradiance reached about 1.0 kW shortly after noon, and wind speed ranged from about 0.5 to 1.3 m/s (Figure 3). Solar irradiances measured with the silicon radiometer closely matched those measured with the first class pyranometer.

From 08:30 to 16:00 LST, each parked car was run through five rounds of soaking and cooling in which an approximately 60 min soak (HVAC off) was followed by about 30 min of maximum cooling. The soaking and cooling intervals were closely synchronized car-to-car.

Simulations (fuel savings and emission reductions)

We used the vehicle simulation tool AVL ADVISOR (version 2004.04.09 SP1) to relate rates of fuel consumption, nitrogen oxide (NO_x) emission, carbon monoxide (CO) emission, and hydrocarbon (HC) emission to ancillary power load. ADVISOR was first developed in November 1994 by National Renewable Energy Laboratory. It was designed as an analysis tool to assist the U.S. Department of Energy (DOE) in quantifying the potential for fuel use and emissions reductions of hybrid electric vehicles. ADVISOR simulates vehicle powertrains and power flows among its components (Wipke et al. 1999a,b). Fuel use and tailpipe emissions can be simulated following various standardized driving cycles. In ADVISOR, AC power load is added as an accessory mechanical load.

In this study we focus on ADVISOR simulations of the EPA Speed Correction (SC03) driving cycle, a transient test cycle with an average speed of 34.8 km/h (21.6 mph) and a maximum speed of 88.2 km/h (54.8 mph). We also show results for the EPA Urban Dynamometer Driving Schedule (UDDS) (average speed = 31.5 km/h = 19.6 mph), and the EPA Highway Fuel Economy Test (HWFET) driving cycle (average speed = 77.7 km/h = 48.3 mph) (EPA 2007). Simulations were performed with ancillary power load ranging from 0 to 4 kW at a resolution of 0.2 kW. Since we did not have access to an ADVISOR vehicle prototype for the Honda Civic, each ADVISOR simulation was run for two available prototypes: one with a 63 kW engine, and the other with a 102 kW engine. Results were then interpolated to match the engine power rating of the Honda Civic GX (84 kW). Note that while the Honda Civic GX is fueled by natural gas, our ADVISOR simulations represent an equal-power vehicle fueled by gasoline. Table 3 presents additional details on the ADVISOR simulations.

We estimate CO_2 emission reduction from fuel savings at the rate of 2321 g CO_2 per L of gasoline (EPA 2005).

We compared ADVISOR fuel economy predictions to EPA gasoline gallon equivalent estimates for the 2009 Honda Civic GX (EPA 2011). EPA estimates are derived from a formula that weights results from five different drive cycles (EPA 2006). ADVISOR simulations of the EPA Urban Dynamometer Driving Schedule (UDDS) and the EPA Highway Fuel Economy Test

(HWFET) were used to estimate city and highway fuel economies, respectively. A "combined" fuel economy was computed as a weighted average (55% UDDS, 45% HWFET).

Table 4 presents results for ancillary loads ranging from 0 to 4 kW. The EPA city, highway, and combined fuel economies lie within the range of our simulation results. We also note that ADVISOR predicts an SC03 drive cycle fuel economy of 19 - 26 mpg, similar to that of the UDDS urban drive cycle.

Results

AC calibration (16 July 2010)

The heater in the silver car was slightly more powerful than that in the black car, yielding 2-3°C higher peak values of vent air temperature and cabin air temperature. However, the AC systems performed comparably: after just 2 min of cooling, the vent air temperatures matched to within 1°C, and the cabin air temperatures agreed to within 0.5°C (Figure 4).

Soaking and cooling (17 July 2010)

Temperatures profiles within each car

Figure 5 shows the evolution of the exterior surface, interior surface, and cabin air temperatures in each car over the course of its five soaking and cooling cycles. The following remarks will focus on the middle three soaking and cooling cycles, which span 10:00 - 14:30 LST and are centered about solar noon (~12:15 LST).

While soaking, the warmest surfaces of the black car are usually its black roof (solar absorptance $A = 1 - \rho$=0.95) and black dashboard (also A=0.95), both of which are directly heated by the sun. Its next warmest surfaces are the ceiling (conductively heated by the roof and radiatively heated by the dashboard and windshield), followed very closely by the windshield (radiatively and convectively heated by the dashboard). The seat, which is heated primarily by radiative exchange with the ceiling, is markedly cooler. The coolest interior surface in the black car is the door, which from geometric considerations can be expected to receive less than half its thermal radiation from the ceiling.

The warmest surfaces of the silver car while soaking are its black dashboard ($A = 0.95$), which is directly heated by the sun, and its windshield, which is radiatively and convectively heated by the dashboard. The next warmest surfaces are its silver roof (directly heated by the sun, but absorbing only 42% of sunlight) and its ceiling (conductively heated by the roof and radiatively heated by the dashboard and windshield). As in the black car, the seat is markedly cooler, and the door is coolest.

We note that in each car, abnormally high door temperatures are observed during the first and last soaking cycles, and abnormally high seat temperatures are seen in the last soaking cycle. This is simply due to direct solar illumination of the door exterior and seat surface, which does not occur at other times.

Air conditioning rapidly cools both the cabin air and all interior surfaces in each vehicle. Dashboard and windshield temperatures remain well above the cabin air temperature because the dashboard is still heated by the sun and the windshield is radiatively coupled to the dashboard. Air conditioning has little effect on roof surface temperature, indicating that the conductive heat flow through the lined ceiling is small compared to the roof's solar heat gain.

We approximate each car's cabin surface temperature T_s as the area-weighted average of its ceiling, dashboard, windshield, seat and door surface temperatures. This estimate of mean interior surface temperature neglects unmonitored surfaces, including the floor, rear window and side windows. Figure 6 shows the evolution of T_s, T_a and T_v in each car, as well as those of $T_a - T_v$ and $T_s - T_a$. (Since the vent air temperature is relevant only when the AC is on, zero values drawn for T_v and $T_a - T_v$ during the soak cycles should be ignored.)

Black car versus silver car

Figure 7 compares the roof, ceiling, dashboard, windshield, seat, door, vent air and cabin air temperatures in the black car to those in the silver car. As expected, the greatest temperature difference is observed at the roof, where the black car was up to 25°C warmer than the silver surface. While soaking, the ceiling temperature difference (black - silver) peaked at 11°C, while the dashboard temperature difference was less than 5°C and the windshield temperature difference was less than 2°C. The seat and door temperature differences reached 7°C and 5°C, respectively. The vent air and cabin air temperature differences each peaked around 5-6°C.

Figure 8 compares the cabin air heating rate dU/dt and AC cooling rate q_{AC} in the black car to those in the silver car. While cooling, the difference in dU/dt is roughly centered about zero and less than 0.03 kW in magnitude. The difference in q_{AC} is much larger, peaking around 0.3 kW. During the cooling cycle, q_{AC} is one to two orders of magnitude larger than dU/dt, suggesting that most of the heat removed by the AC comes from the cabin surface, rather than the cabin air.

Cooldown temperature versus soak temperature

The five cooling cycles are denoted “cool1” through “cool5”. Table 5 summarizes the properties of each cooling cycle, including its start and end time, duration, primary weather conditions, cabin air and surfaces temperatures after soaking and after cooling, and vent air temperatures

after cooling. Each temperature is reported first for the black car, then for the silver car, followed by the black - silver temperature difference.

The cabin air and vent air temperatures attained after ~30 min of cooling each strongly and linearly correlate to the cabin air temperature reached after ~60 min of soaking, with coefficient of determination R^2>0.99 for the former and R^2=0.95 for the latter (Figure 9a). The (area weighted mean) cabin surface temperatures attained after soaking and after cooling also linearly correlate to the cabin air soak temperature, with R^2=0.87 and R^2=0.93, respectively (Figure 9b). The same linear relationships work equally well for both cars. This indicates that under the strictly controlled conditions of these experiments, cabin air soak temperature captures the thermal history of the soaking interval sufficiently well to predict cabin air and cabin surface temperatures after cooling.

Applicability of cabin air temperature model

The validity of the cabin air temperature model in Eq. (2) was tested by regressing the rate of change of the cabin air temperature, dT_a/dt, to the temperature differences $T_v - T_a$ and $T_s - T_a$. Regression coefficients α and β for each car and cooling cycle are presented in Table 6, along with each fit's coefficient of determination R^2. Values of R^2 were fairly high, ranging from 0.86 to 0.93 for the black car and 0.86 to 0.95 for the silver car. Figure 10 shows the measured and fitted values of dT_a/dt for the fourth cooling cycle in each car.

Figure 11 shows the variation with cooling time of the cabin air temperature reduction $T_a(0) - T_a(t)$ in each vehicle. Cooling is rapid at the start of each 30 min cycle and slow near its end. For example, during the fourth cooling cycle, the cabin air temperature in the black car falls 16°C in the first two minutes (8°C/min), another 11°C in the next 18 minutes (0.6°C/min), and just 2°C in the final 10 minutes (0.2°C/min). This indicates that T_a asymptotically approaches a quasi-steady value T_a^* toward the end of the cooling cycle.

Figure 12 shows the variation with cooling time of $T_s - T_a$ in each car. In the three middle cooling cycles (cool2, cool3 and cool4), this temperature difference varies little after the first two minutes of cooling. For example, during the final 28 minutes of the fourth cooling cycle, $T_s - T_a$ decreases by 1.2°C in the black car and 0.5°C in the silver car, while the vent air temperatures each fall by about 7°C. This indicates that $T_s - T_a$ depends only weakly on T_v.

Resizing AC to attain 25°C final cabin air temperature

The black car attained a final cabin air temperature below 25°C in the first cooling cycle, and the silver car did so in the first and second cooling cycles. Otherwise, neither vehicle's cabin air

temperature was reduced to 25°C or lower after approximately 30 min of maximum cooling. For example, at the end of the fourth cooling cycle, the cabin air temperatures in the black and silver cars were 34.3°C and 29.9°C, respectively (Table 6).

To attain a lower final cabin air temperature $T_a'^*$, Eq. (4) indicates that the vent air temperature $T_v(t)$ must be decreased by the difference ΔT between the cabin air final temperature T_a^* (approximated by the cabin air temperature measured at the end of the cooling cycle) and $T_a'^*$. For example, in the fourth cooling cycle ΔT would be 9.3°C for the black car and 4.9°C for the silver car if $T_a'^*$=25°C.

New vent air temperature profiles $T_v'(t) \equiv T_v(t) - \Delta T$ were computed for each car and cooling cycle based on the value of ΔT required to cool the cabin air to 25°C. Eq. (5) was then numerically integrated to compute the new cabin air temperature profile $T_a'(t)$. Figure 13 compares the measured and fitted values of $T_a(t)$ in the fourth cooling cycle to the values of $T_a'(t)$ computed after decreasing the black and silver cars' vent air temperatures by ΔT=9.3°C and ΔT=4.9°C, respectively. Also drawn for reference is the cooldown target temperature (25°C).

AC cooling rates before and after vent temperature reduction were computed from Eqs. (6) and (7). Figure 14 shows for the fourth cooling cycle in each car the measured AC cooling rate and the AC cooling rate after lowering the vent air temperature to attain a final cabin air temperature of 25°C.

The AC cooling capacity Q (peak AC cooling rate) required to attain $T_a'^*$=25°C was computed from Eq. (8) for each car and cooling cycle (Table 6). For example, in the fourth cooling cycle Q was 3.83 kW in the black car, and 3.34 kW in the silver car. The ratio of Q_{silver} to Q_{black} ranged from 0.83 to 0.87 over the three middle cooling cycles.

Fuel savings and emission reductions

Fuel consumption and pollutant emission versus ancillary power load

Table 7 shows values of γ obtained by linearly regressing ADVISOR simulations of fuel consumption, NO_x emission, CO emission and HC emission rates to ancillary power load. The variations of fuel consumption and emissions with ancillary load were highly linear within the simulated range (0-4 kW) and the minimum coefficient of determination (R^2) was 0.96. Figure 15 relates reductions in fuel consumption and emission to the ancillary loads of the standard

(black) and cool (nonblack) cars. Each curve represents a different value for ancillary load of the standard car. For brevity, we present charts only for the SC03 driving cycle.

Fuel savings and emission reductions versus cool car solar reflectance

Since roof and cabin air soak temperatures peaked in the fourth cycle (Table 5), AC capacity requirements Q_L (black car) and Q_H (silver car) were based on values computed for the fourth cooling cycle. The following analysis assumes AC capacities Q_L = 3.83 kW and Q_H = 3.34 kW and shell solar reflectances ρ_L =0.05 and ρ_H =0.58, for a capacity reduction of 92.5 W per 0.1 increase in shell solar reflectance.

Hendricks (2001b) obtained a maximum COP of 1.6 when optimizing the COP of a mechanically driven compressor for the SC03 cycle. Here we select a COP of 2 to conservatively estimate reduction in ancillary power load, which is inversely proportional to COP.

Table 8, Figure 16, and Figure 17 present fuel savings and emissions reductions attained when a cool (solar reflective) car shell is substituted for a standard (black) car shell (ρ =0.05). Dashed vertical lines in Figure 16 and Figure 17 mark the shell solar reflectances of a typical cool colored car (ρ =0.35), a typical white or silver car (ρ =0.60), and a hypothetical super-white car (ρ =0.80). Figure 16 shows fractional fuel savings and emissions reductions and Figure 17 shows absolute fuel savings and emissions reductions.

Results from our model with γ values from the SC03 drive cycle indicate selecting a typical cool colored shell (ρ =0.35) would reduce fuel consumption by 0.12 L per 100 km (1.1%), increasing fuel economy by 0.10 km L^{-1} [0.24 mpg] (1.1%). It would also decrease CO_2 emissions by 2.7 g km^{-1} (1.1%), NO_x emissions by 5.4 mg km^{-1} (0.44%), CO emissions by 17 mg km^{-1} (0.43%), and HC emissions by 4.1 mg km^{-1} (0.37%). Selecting a typical white or silver shell (ρ = 0.60) instead of a black shell would lower fuel consumption by 0.21 L per 100 km (1.9%), raising fuel economy by 0.19 km L^{-1} [0.44 mpg] (2.0%). It would also decrease CO_2 emissions by 4.9 g km^{-1} (1.9%), NO_x emissions by 9.9 mg km^{-1} (0.80%), CO emissions by 31 mg km^{-1} (0.79%), and HC emissions by 7.4 mg km^{-1} (0.67%). A hypothetical super-white car shell[4] (ρ = 0.80) could save 0.29 L per 100 km (2.6%), increasing fuel economy by 0.25 km L^{-1} [0.59 mpg] (2.7%) and decreasing CO_2, NO_x, CO and HC emissions by 6.7 g km^{-1} (2.6%), 13 mg km^{-1} (1.1%), 43 mg km^{-1} (1.1%), and 10 mg km^{-1} (0.91%), respectively.

[4] Many white metal roofing products have initial solar reflectances in the range of 0.7 - 0.8 (CRRC 2011). We present the super-white shell (ρ = 0.80) as a limiting case.

As discussed previously, emissions in standardized driving cycles are typically lower than those in real-world (off-cycle) driving. Hence, our simulation results may underestimate emission reductions.

We can compare fuel and emissions reductions of urban versus highway driving by observing results for the UDDS and HWFET driving cycles (Figure 16). Relative to the SC03 drive cycle, fuel savings are larger for the UDDS cycle (urban driving) and smaller for the HWFET cycle (highway driving). Further, relative to the SC03 cycle, emissions reductions for NO_x, CO, and HC are smaller for both the UDDS cycle and HWFET cycle. Emissions reductions are larger for UDDS than HWFET for NO_x, CO, and HC. This may be due to the fact that emissions are more sensitive to transients (e.g., simulated vehicle accelerations) in driving cycles (Samuel et al. 2002).

Summary

In this study we estimated the decrease in soak temperature, potential reduction in AC capacity, and potential fuel savings and emission reductions attainable through the use of solar reflective shells. First, we experimentally characterized component temperatures and cooling demands in a pair of otherwise identical dark and light colored vehicles, the former with low solar reflectance ($\rho = 0.05$) and the latter with high solar reflectance ($\rho = 0.58$). Second, we developed a thermal model that predicted the AC capacity required to cool each vehicle to a comfortable final temperature of 25°C within 30 minutes. Third, we used the ADVISOR vehicle simulation tool to estimate the fuel consumption and pollutant emissions of each vehicle in various standard drive cycles (SC03, UDDS, and HWFET). Finally, we calculated the fuel savings and emission reductions attainable by using a cool shell to reduce ancillary load.

The air conditioners in the experimental vehicles were in most trials too small to lower cabin air temperature to 25°C within 30 minutes. We estimate that if the vehicle ACs were resized to meet this target, the AC cooling capacity would be 3.83 kW for the car with low solar reflectance and 3.34 kW for the car with high solar reflectance (Table 6).

Assuming that potential reductions in AC capacity and engine ancillary load scale linearly with increase in shell solar reflectance, ADVISOR simulations of the SC03 driving cycle indicate that substituting a typical cool-colored shell ($\rho = 0.35$) for a black shell ($\rho = 0.05$) would reduce fuel consumption by 0.12 L per 100 km (1.1%), increasing fuel economy by 0.10 km L^{-1} [0.24 mpg] (1.1%). It would also decrease CO_2 emissions by 2.7 g km^{-1} (1.1%), NO_x emissions by 5.4 mg km^{-1} (0.44%), CO emissions by 17 mg km^{-1} (0.43%), and HC emissions by 4.1 mg km^{-1} (0.37%). Selecting a typical white or silver shell ($\rho = 0.60$) instead of a black shell would lower fuel consumption by 0.21 L per 100 km (1.9%), raising fuel economy by 0.19 km L^{-1} [0.44 mpg] (2.0%). It would also decrease CO_2 emissions by 4.9 g km^{-1} (1.9%), NO_x emissions by 9.9 mg km^{-1} (0.80%), CO emissions by 31 mg km^{-1} (0.79%), and HC emissions by 7.4 mg km^{-1} (0.67%).

A hypothetical super-white car shell ($\rho = 0.80$) could save 0.29 L per 100 km (2.6%), increasing fuel economy by 0.25 km L^{-1} [0.59 mpg] (2.7%) and decreasing CO_2, NO_x, CO and HC emissions by 6.7 g km^{-1} (2.6%), 13 mg km^{-1} (1.1%), 43 mg km^{-1} (1.1%), and 10 mg km^{-1} (0.91%), respectively. These results may underestimate emission reductions in real-world driving.

Acknowledgments

This work was supported by the California Energy Commission through its Public Interest Energy Research Program. It was also supported by the Assistant Secretary for Energy Efficiency and Renewable Energy, Office of Building Technology, State, and Community Programs, of the U.S. Department of Energy under Contract No. DE-AC02-05CH11231. We wish to thank the California Department of General Services for use of their vehicles and facility, with special appreciation to Kimberly Harbison for her assistance; John Rugh of the National Renewable Energy Laboratory, for technical advice; and Philip Misemer of the California Energy Commission, for guiding our project.

References

Akabane, T., S. Ikeda, K. Kikuchi, Y. Tamura, R. Sakano, W. Bessler, and H. Harms. 1989. Evaluation of an electrically driven automotive air conditioning system using a scroll hermetic compressor with a brushless DC Motor, SAE Technical Paper 890308, DOI: 10.4271/890308.

Bevilacqua, O.M. 1999. Effect of air conditioning on regulated emissions for in-use vehicles. Clean Air Vehicle Technology Center, Oakland, CA. Phase I final report prepared for Coordinating Research Council, Inc. Atlanta, GA, CRC Project E-37, October.

Bharathan, D., L. Chaney, R.B. Farrington, J. Lustbader, M. Keyser and J. Rugh. 2007. An overview of vehicle test and analysis from NREL's A/C fuel use reduction research. Paper presented at Vehicle Thermal Management Systems Conference & Exhibition (VTMS-8), May 20-24, Nottingham, UK.

Carslaw, H.S., and J.C. Jeager. 1959. *Conduction of Heat in Solids*, 2nd ed. Clarendon Press, Oxford.

Clear, R.D, L. Gartland and F.C. Winkelmann. 2003. An empirical correlation for the outside convective air-film coefficient for horizontal roofs, *Energy & Buildings* 35, 797-811.

CRRC. 2011. Cool Roof Rating Council Rated Products Directory. Online at http://coolroofs.org .

Cullimore, B.A., and T.J. Hendricks. 2001. Design and transient simulation of vehicle air conditioning systems. Paper presented at Vehicle Thermal Management Systems Conference & Exhibition, May, Nashville, TN, USA.

Daly, S. 2006. *Automotive air-conditioning and climate control systems*. Butterworth-Heinemann, Lincare House, Jordan Hill, Oxford OX2 8DP, 30 Corporate Drive, Suite 400 Burlington, MA 01803.

EPA. 2005. Emission facts: average carbon dioxide emissions resulting from gasoline and diesel fuel. Office of Transportation and Air Quality, U.S. Environmental Protection Agency. EPA-420-F-05-001, February.

EPA. 2006. Fuel economy labeling of motor vehicle revisions to improve calculation of fuel economy estimates. Final technical support document. U.S. Environmental Protection Agency. Office of Transportation and Air Quality. EPA420-R-06-017.

EPA. 2007. Federal Test Procedure Revisions: Driving Cycles. Office of Transportation and Air Quality, U.S. Environmental Protection Agency. Online Resource. http://www.epa.gov/oms/sftp.htm#cycles. Accessed December, 2010.

EPA. 2009. Draft Regulatory Impact Analysis: Proposed Rulemaking to Establish Light-Duty Vehicle Greenhouse Gas Emission Standards and Corporate Average Fuel Economy Standards. Assessment and Standards Division, Office of Transportation and Air Quality, U.S. Environmental Protection Agency. EPA-420-D-09-003, September.

EPA. 2011. www.fueleconomy.gov. US Environmental Protection Agency and U.S. Department of Energy. Online at http://fueleconomy.gov .

Han, T., and K.H. Chen. 2009. Assessment of various environmental thermal loads on passenger compartment soak and cool-down analyses. Paper presented at SAE World Congress & Exhibition, April, Detroit, MI, USA.

Hassan, K., and S.A. Mohamed. 1970. Natural convection from isothermal flat surfaces. *International Journal of Heat and Mass Transfer* 13 (12), 1873-1886.

Hendricks, T.J. 2001a. Optimization of vehicle air conditioning systems using transient air conditioning performance analysis. Paper presented at Vehicle Thermal Management Systems Conference & Exposition, May, Nashville, TN, USA.

Hendricks, T.J. 2001b. Vehicle transient air conditioning analysis: Model development & system optimization investigations. Golden, Colorado, USA: NREL/TP-540-30715. http://www.nrel.gov/docs/fy01osti/30715.pdf .

Henry, R.R., J. Koo and C. Richter. 2001. Model development, simulation and validation, of powertrain cooling system for a truck application. Paper presented at Vehicle Thermal Management Systems Conference & Exposition, Nashville, TN, USA.

Heydari, A., and S. Jani. 2001. Entropy-minimized optimization of an automotive air conditioning and HVAC system. Paper presented at SAE World Congress, March, Detroit, MI, USA.

Hoke, P.B., and C. Greiner. 2005. Vehicle paint radiation properties and affect on vehicle soak temperature, climate control system load, and fuel economy. Paper presented at SAE World Congress & Exhibition, April, Detroit, MI, USA.

Huang, D., M.S. Wallis, E. Oker and S. Lepper. 2007. Design of vehicle air conditioning systems using heat load analysis. Paper presented at SAE World Congress & Exhibition, April, Detroit, MI, USA.

Junior, C. S., N.C. Strupp, N. C. Lemke and J. Koehler. 2009. Modeling a thermoelectric HVAC system for automobiles. *Journal of Electronic Materials* 38 (7), 1093-1097.

Konopacki, S., H. Akbari, M. Pomerantz, S. Gabersek and L. Gartland. 1997. Cooling energy savings potential of light-colored roofs for residential and commercial buildings in 11 US metropolitan areas. Technical Report LBNL-39433, Lawrence Berkeley National Laboratory, Berkeley, CA.

Kyle, D.M., V.C. Mei and F.C. Chen. 1993. An automobile air conditioning design model. Paper presented at Vehicle Thermal Management System Conference, March, Columbus, OH, USA.

Levinson, R., H. Akbari and P. Berdahl. 2010a. Measuring solar reflectance—Part I: defining a metric that accurately predicts solar heat gain. *Solar Energy* 84, 1717-1744.

Levinson, R., H. Akbari and P. Berdahl. 2010b. Measuring solar reflectance—Part II: review of practical methods. *Solar Energy* 84, 1745-1759.

Rugh, J. P., T.J. Hendricks and K. Koram. 2001. Effect of solar reflective glazing on Ford Explorer climate control, fuel economy, and emissions. Paper presented at International Body Engineering Conference & Exposition, October, Detroit, MI, USA.

Rugh, J. 2002. Integrated numerical modeling process for evaluating automobile climate control systems. Paper presented at Future Car Congress, June, Crystal City, VA, USA.

Rugh, J.P., and V.S. Malaney. 2004. Comparison of indoor vehicle thermal soak tests to outdoor tests. Paper presented at Future Car Congress, April, Crystal City, VA, USA.

Rugh, J., and R. Farrington. 2008. Vehicle ancillary load reduction project close-out report: An overview of the task and a compilation of the research results. Golden, CO: National Renewable Energy Laboratory (NREL), NREL/TP-540-42454.

Samuel, S., L. Austin, and D. Morrey. 2002. Automotive test drive cycles for emission measurement and real-world emission levels – a review. *Proceedings Institution of Mechanical Engineers.* 216, 555-564.

Sullivan, R., and S. Selkowitz. 1990. Effects of Glazing and Ventilation Options on Automobile Air Conditioner Size and Performance. Paper presented at SAE International Congress and Exposition. February, Detroit, MI, USA.

Taxis-Reischl, B., S. Morgenstern, T. Mersch and F. Brotz. 2001. Progress in the optimized application of simulation tools in vehicle air conditioning. Paper presented at Vehicle Thermal Management Systems Conference & Exposition, May, Nashville, TN, USA.

Turler, D., D. Hopkins and H. Goudey. 2003. Reducing vehicle ancillary loads using advanced thermal insulation and window technologies. Paper presented at SAE World Congress & Exhibition, Detroit, MI, USA.

Wipke, K.M., Cuddy, D. Bharathan, S. Burch, V. Johnson, A. Markel and S. Sprik. 1999a. ADVISOR 2.0: A Second-Generation Advanced Vehicle Simulatory for Systems Analysis. 14 pp. NREL Report No. TP-540-25928, Golden, CO: NREL.

Wipke, K., M. Cuddy and S. Burch. 1999b. ADVISOR 2.1: A user-friendly advanced powertrain simulation using a combined backward/forward approach. 14 pp. NREL Report No. JA-540 26839, Golden, CO: NREL.

Wolfahrt, J., W. Baier, B. Wiesler, A. Raulot, J. Rugh, D. Bharathan and C. Kussman. 2005. Aspects of cabin fluid dynamics, heat transfer, and thermal comfort in vehicle thermal management simulations. Paper presented at Vehicle Thermal Management Systems Conference & Exposition, May, Toronto, ON, Canada.

Zhang, H., L. Dai, G. Xu, Y. Li, W. Chen and W. Tao. 2009a. Studies of air-flow and temperature fields inside a passenger compartment for improving thermal comfort and saving energy. Part I: Test/numerical model and validation. *Applied Thermal Engineering* 29 (7), 2022-2027.

Zhang, H., L. Dai, G. Xu, Y. Li, W. Chen and W. Tao. 2009b. Studies of air-flow and temperature fields inside a passenger compartment for improving thermal comfort and saving energy. Part II: Simulation results and discussion. *Applied Thermal Engineering* 29 (7), 2028-2036.

Table 1. General properties of test vehicles.

make and model	2009 Honda Civic 4DR GX	
cabin volume (m^3)	2.57	
engine idle speed (RPM)	700	
AC air flow rate (m^3/s)	0.1	
	black	*silver*
odometer distance (mi) [km]	4300 [6900]	6200 [10000]
AC line high pressure (psi) [MPa]	165 [1.13]	175 [1.20]
AC line low pressure (psi) [MPa]	35 [0.24]	40 [0.28]

Table 2. Vehicle surface properties.

surface	**area (m^2)**	**solar reflectance**	**thermal emittance**
roof	2.0	0.05 (black) 0.58 (silver)	0.83 (black) 0.79 (silver)
ceiling	2.0	0.41	n/a
dashboard	0.6	0.06	n/a
windshield	0.9	0.06	0.88
seat	2.4	0.38	n/a
door	3.0	0.11	n/a

Table 3. Input parameters for the two vehicle prototypes simulated with ADVISOR. Simulation results from these two cars were interpolated to match the 84 kW power rating of the Honda Civics used in our experiments.

	prototype 1	**prototype 2**
vehicle type	compact	compact
vehicle power rating (kW)	63	102
vehicle mass (kg)	1466	1601
drivetrain configuration	conventional	conventional
fuel converter	FC_SI63_emis	FC_SI102_emis

Table 4. US EPA (2011) and ADVISOR fuel economy (mpg) estimates for the 2009 Honda Civic GX.

	EPA sticker	ADVISOR (0 - 4 kW ancillary load)
City	24	19 - 27
Highway	36	31 - 39
Combined city/highway	28	24 - 32

Table 5. Cooling trial measurements. Temperature differences are black car - silver car.

cycle	**cool1**	**cool2**	**cool3**	**cool4**	**cool5**
start (LST)	09:32	11:02	12:33	14:02	15:32
end (LST)	09:59	11:32	13:01	14:32	16:00
duration (min)	28	30	28	30	28
mean outdoor air temperature (°C)	25.0	28.8	32.9	35.8	37.5
mean solar irradiance (kW/m^2)	0.83	0.98	1.00	0.86	0.64
black cabin air temperature after soaking (°C)	47.7	55.9	61.8	64.4	63.6
silver cabin air temperature after soaking (°C)	43.3	50.7	56.1	58.0	57.3
cabin air temperature difference after soaking (°C)	4.4	5.2	5.7	6.4	6.4
black cabin air temperature after cooling (°C)	22.1	27.7	32.0	34.3	33.7
silver cabin air temperature after cooling (°C)	19.6	24.9	28.2	29.9	29.5
cabin air temperature difference after cooling (°C)	2.5	2.8	3.8	4.4	4.2
black cabin surface temperature after soaking (°C)	48.5	53.3	58.0	62.2	66.0
silver cabin surface temperature after soaking (°C)	45.3	48.4	52.5	56.4	59.9
cabin surface temperature difference after soaking (°C)	3.2	4.9	5.5	5.8	6.1
black cabin surface temperature after cooling (°C)	28.7	33.7	38.3	40.9	42.7
silver cabin surface temperature after cooling (°C)	27.4	30.5	34.2	36.5	38.3
cabin surface temperature difference after cooling (°C)	1.3	3.2	4.1	4.4	4.4
black vent air temperature after cooling (°C)	9.6	14.2	17.4	20.5	20.2
silver vent air temperature after cooling (°C)	9.1	13.0	15.4	16.8	17.0
vent air temperature difference after cooling (°C)	0.5	1.2	2.0	3.7	3.2

Table 6. Characteristics of each cooling trial, including fit parameters α and β; coefficient of determination R^2; measured final cabin air temperature T_a^*; and AC cooling capacity Q needed to attain a final cabin air temperature of 25°C.

trial	α [s^{-1}]	β [s^{-1}]	R^2	T_a^* [°C]	Q [kW]
black_cool1	0.017	0.030	0.86	22.1	2.60
black_cool2	0.012	0.024	0.90	27.7	3.05
black_cool3	0.010	0.023	0.88	32.0	3.66
black_cool4	0.012	0.024	0.93	34.3	3.83
black_cool5	0.015	0.022	0.93	33.7	3.64
silver_cool1	0.018	0.025	0.95	19.6	2.35
silver_cool2	0.012	0.024	0.86	24.9	2.61
silver_cool3	0.011	0.023	0.90	28.2	3.03
silver_cool4	0.011	0.023	0.89	29.9	3.34
silver_cool5	0.015	0.022	0.90	29.5	3.25

Table 7. Coefficients of proportionality γ relating changes in rates of fuel consumption F, NO_x emission E_{NO_x}, CO emission E_{CO} and HC emission E_{HC} in each of three drive cycles to change in ancillary power load.

Coefficient	**UDDS**	**SC03**	**HWFET**
γ_F (L per 100km per kW)	0.884	0.830	0.403
γ_{E,NO_x} (mg km^{-1} kW^{-1})	33	39	24
$\gamma_{E,CO}$ (mg km^{-1} kW^{-1})	60	123	29
$\gamma_{E,HC}$ (mg km^{-1} kW^{-1})	22	29	10

Table 8. Variations with shell solar reflectance of rates of fuel consumption, fuel savings, pollutant emission and emission reduction for a compact sedan (engine power 84 kW). Results are presented for three different drive cycles simulated using ADVISOR. Parenthetical results indicate percent reductions in fuel consumption and emission rates relative to the black car.

	Driving Cycle	Black car (ρ = 0.05)	Cool colored car (ρ = 0.35)	Silver or white car (ρ = 0.60)	Hypothetical super-white car (ρ = 0.80)
Fuel consumption (L per 100 km)					
	SC03 [a]	10.95	10.84	10.74	10.67
	UDDS [b]	10.59	10.46	10.36	10.28
	HWFET [c]	6.86	6.80	6.76	6.72
Fuel savings (L per 100 km)					
	SC03	NA	0.12 (1.1%)	0.21 (1.9%)	0.29 (2.6%)
	UDDS	NA	0.12 (1.2%)	0.23 (2.1%)	0.31 (2.9%)
	HWFET	NA	0.056 (0.82%)	0.10 (1.5%)	0.14 (2.0%)
CO_2 emission reduction (g km^{-1}) [d]					
	SC03	NA	2.7	4.9	6.7
	UDDS	NA	2.9	5.2	7.1
	HWFET	NA	1.3	2.4	3.3
NO_x emission (g km^{-1})					
	SC03	1.22	1.22	1.22	1.21
	UDDS	0.70	0.69	0.69	0.69
	HWFET	0.53	0.53	0.53	0.52
NO_x emission reduction (mg km^{-1})					
	SC03	NA	5.4 (0.44%)	9.9 (0.80%)	13 (1.1%)
	UDDS	NA	4.7 (0.67%)	8.5 (1.2%)	12 (1.7%)
	HWFET	NA	3.3 (0.62%)	6.1 (1.1%)	8.3 (1.6%)
CO emission (g km^{-1})					
	SC03	3.99	3.98	3.96	3.95
	UDDS	2.07	2.06	2.06	2.05
	HWFET	1.69	1.69	1.69	1.68
CO emission reduction (mg km^{-1})					
	SC03	NA	17 (0.43%)	31 (0.79%)	43 (1.07%)
	UDDS	NA	8.4 (0.41%)	15 (0.74%)	21 (1.01%)
	HWFET	NA	4.0 (0.24%)	7.3 (0.43%)	10 (0.59%)

(table continues next page)

	Driving Cycle	Black car (ρ = 0.05)	Cool colored car (ρ = 0.35)	Silver or white car (ρ = 0.60)	Hypothetical super-white car (ρ = 0.80)
HC emission (g km^{-1})					
	SC03	1.12	1.11	1.11	1.11
	UDDS	0.61	0.61	0.61	0.60
	HWFET	0.46	0.46	0.46	0.46
HC emission reduction (mg km^{-1})					
	SC03	NA	4.1 (0.37%)	7.4 (0.67%)	10 (0.91%)
	UDDS	NA	3.1 (0.50%)	5.6 (0.92%)	7.6 (1.3%)
	HWFET	NA	1.4 (0.30%)	2.5 (0.55%)	3.4 (0.75%)

[a] SC03 simulates transient driving (average speed = 34.8 km/h, 21.6 mph).

[b] UDDS simulates urban driving (average speed = 31.5 km/h = 19.6 mph).

[c] HWFET simulates highway driving (average speed = 77.7 km/h = 48.3 mph).

[d] CO_2 emission reduction calculated at the rate of 2321 g CO_2 per L gasoline (EPA 2005).

Figure 1. Experimental vehicles parked facing south in Sacramento, CA on July 17, 2010. Tower between vehicles (black car, solar reflectance 0.05, left; silver car, solar reflectance 0.58, right) supports a Davis Instruments Vantage Pro weather station (upper mount) and an Eppley Laboratory Precision Spectral Pyranometer (lower mount).

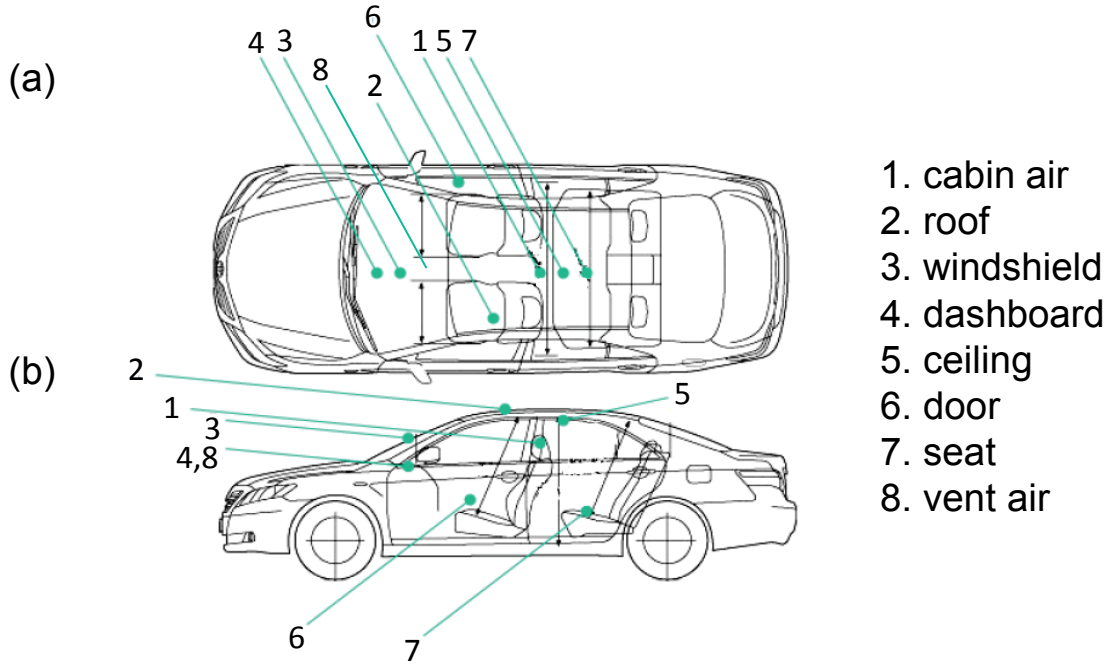

Figure 2. Locations of the eight cabin temperature sensors (thermistors), shown in (a) top view and (b) side view.

(a)

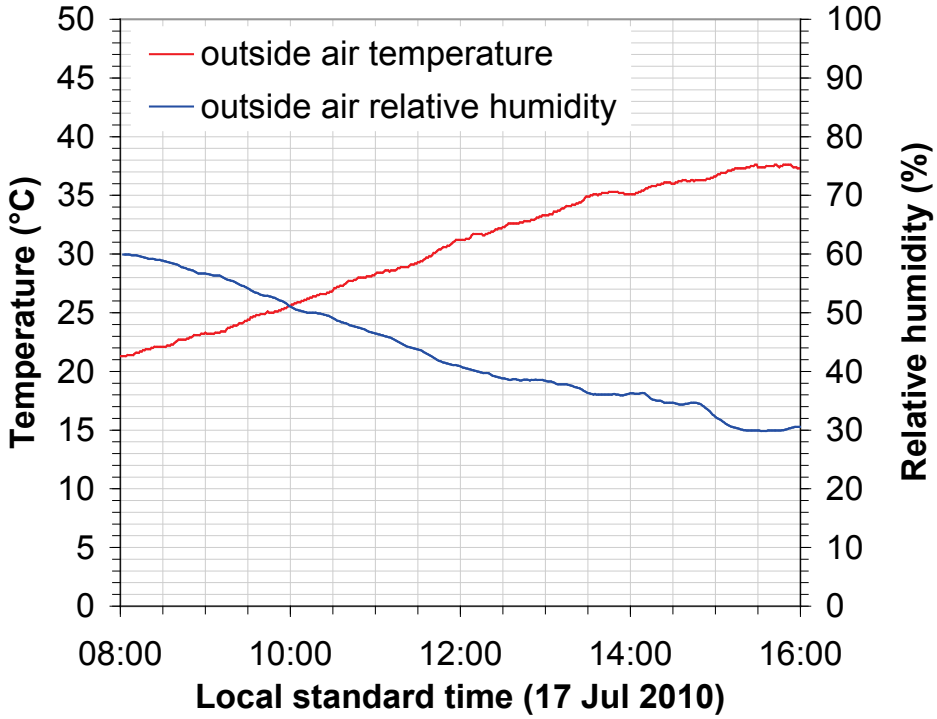

(b)

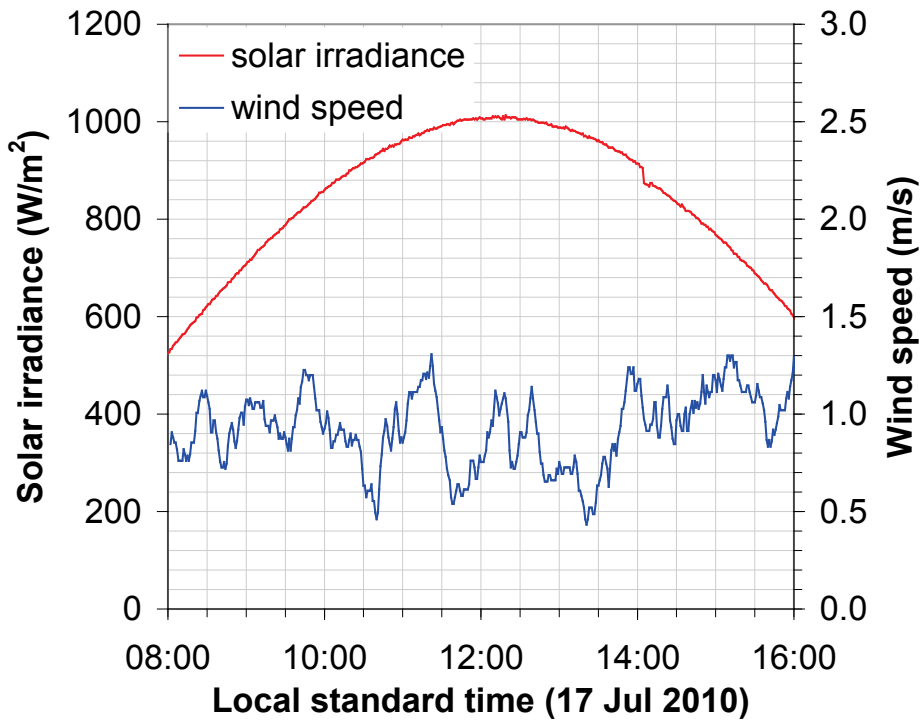

Figure 3. Weather during soaking and cooling trials, including (a) outdoor air temperature and humidity and (b) global horizontal solar irradiance and wind speed.

(a)

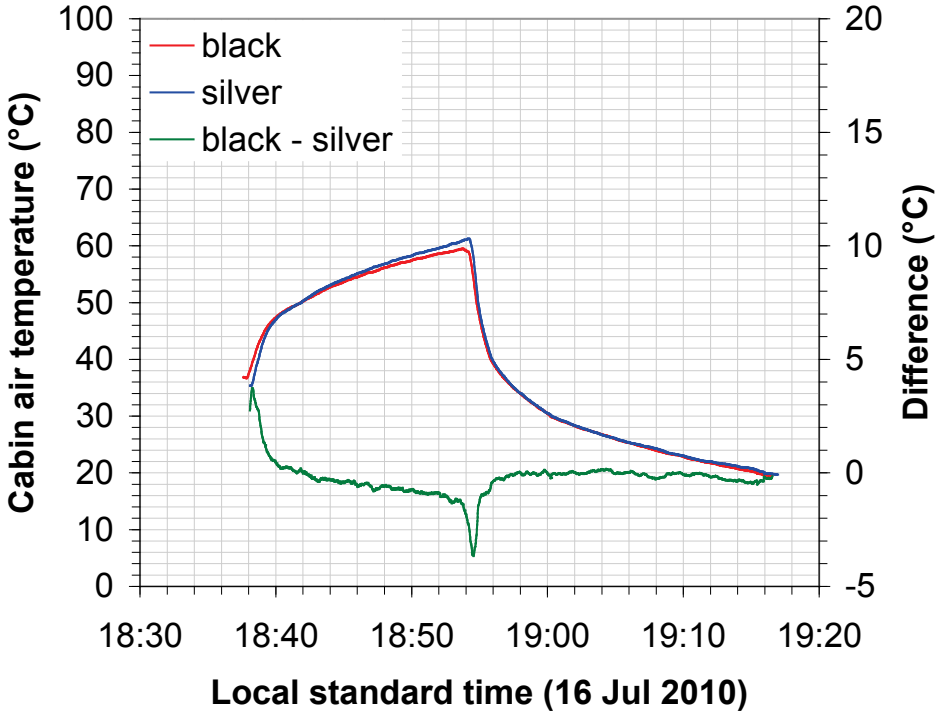

(b)

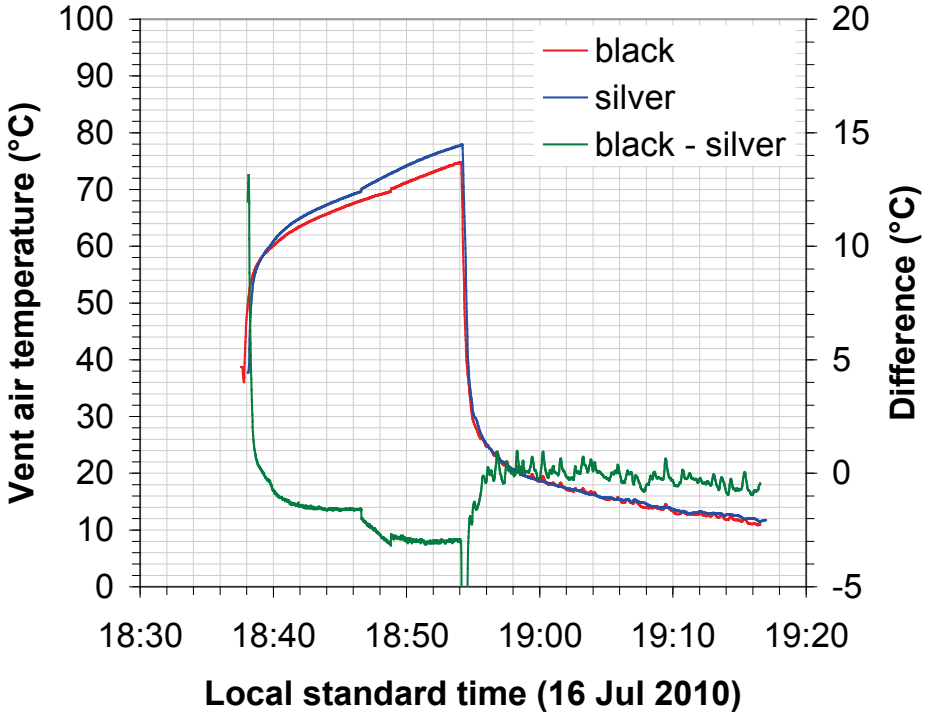

Figure 4. Comparisons of (a) cabin air temperature and (b) vent air temperature in each car during indoor HVAC calibration.

(a)

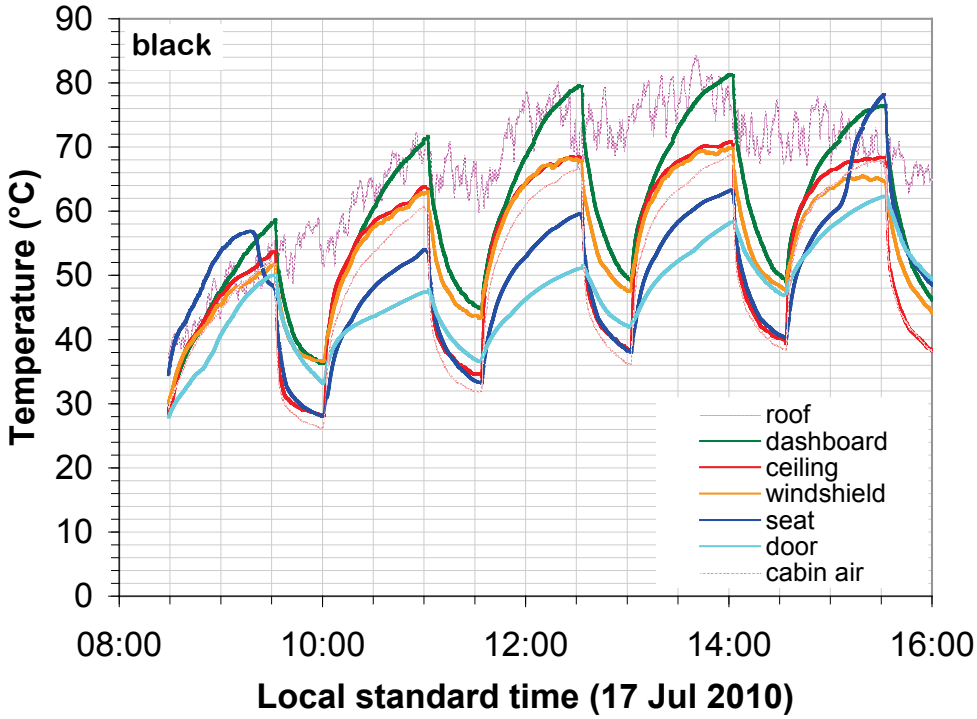

(b)

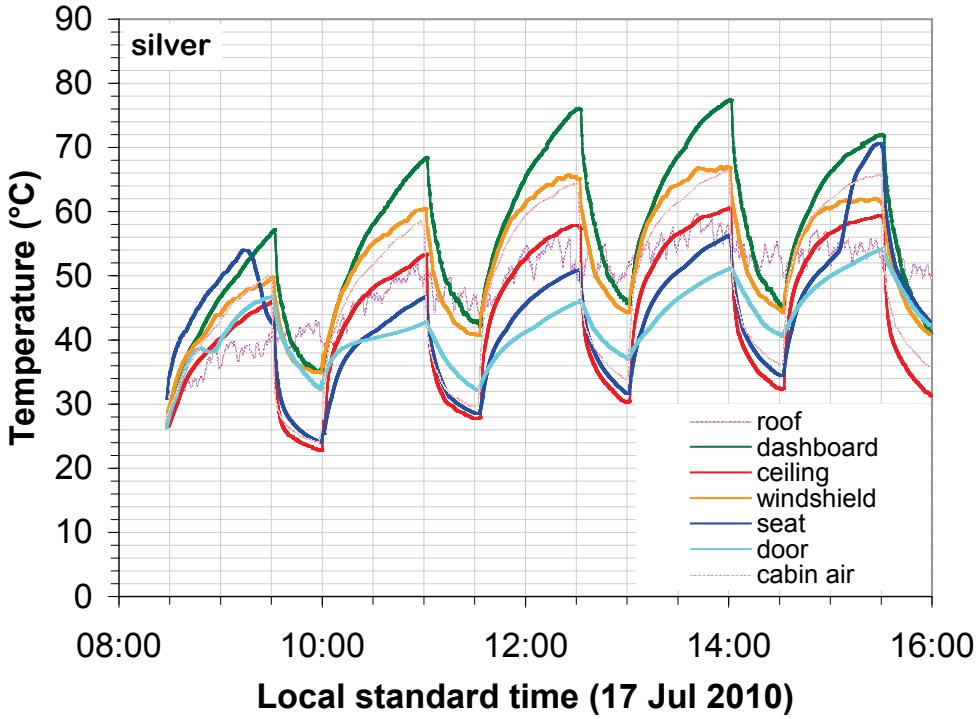

Figure 5. Roof, dashboard, ceiling, windshield, seat, door and cabin air temperatures measured during soaking and cooling trials in (a) the black car and (b) the silver car.

(a)

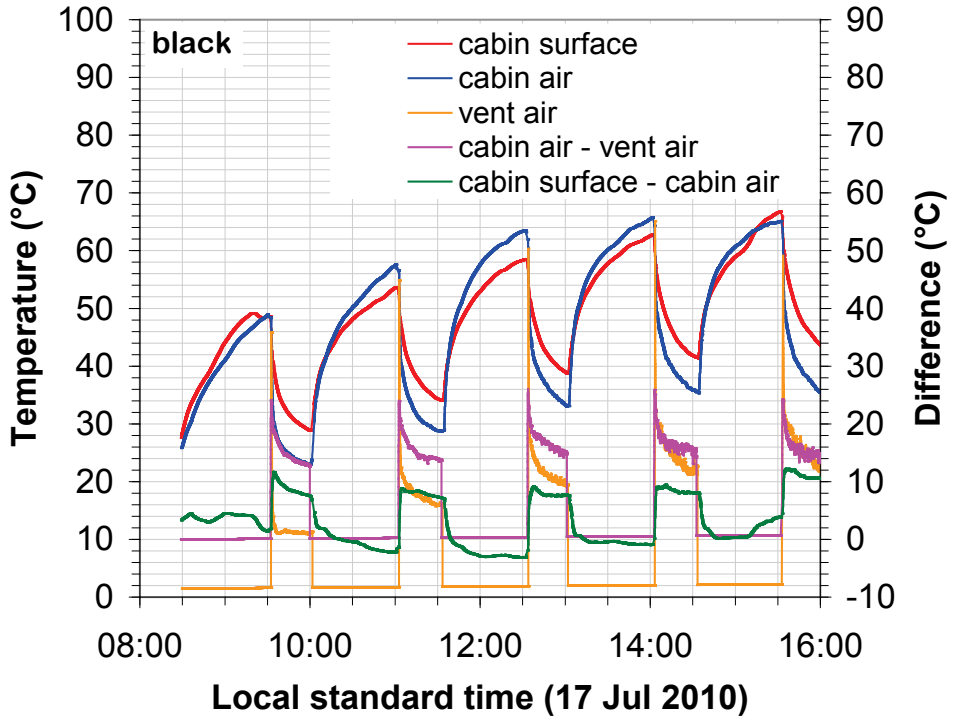

(b)

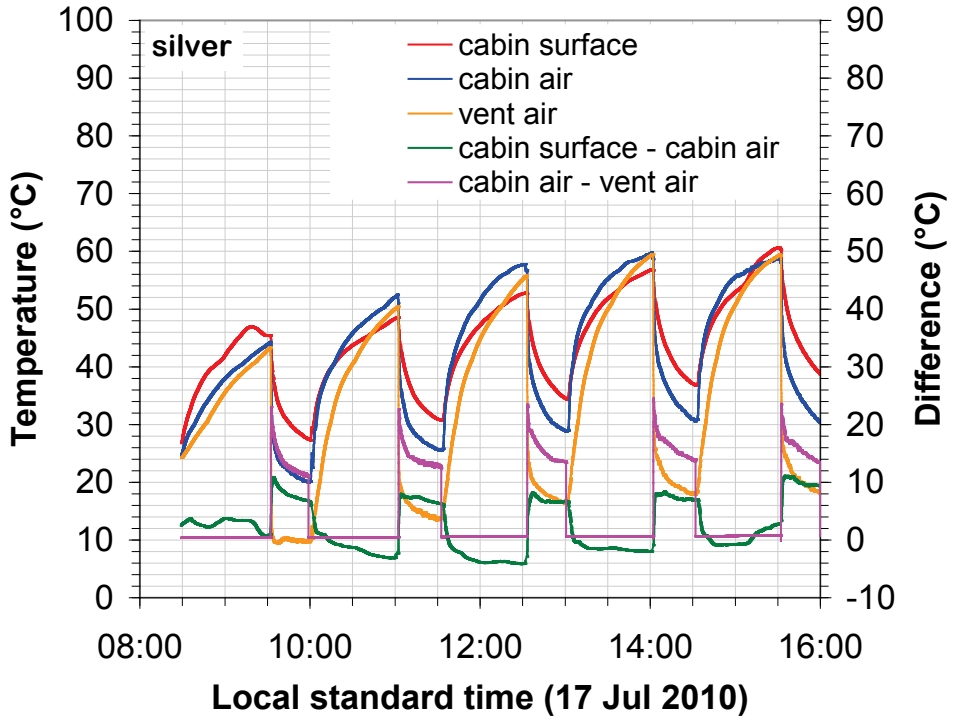

Figure 6. Cabin surface, cabin air and vent air temperatures measured during soaking and cooling trials in (a) the black car and (b) the silver car. Also shown are differences between cabin surface and cabin air temperature and between cabin air and vent air temperature.

(a)

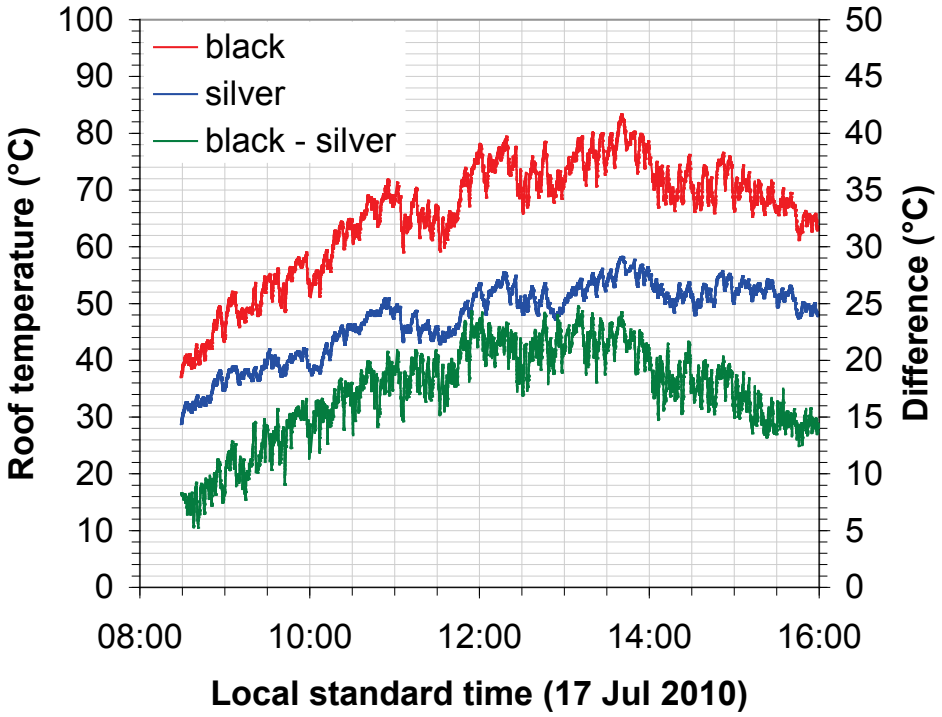
black
silver
black - silver
Roof temperature (°C)
Difference (°C)
100
90
80
70
60
50
40
30
20
10
0
50
45
40
35
30
25
20
15
10
5
0
08:00
10:00
12:00
14:00
16:00
Local standard time (17 Jul 2010)

(b)

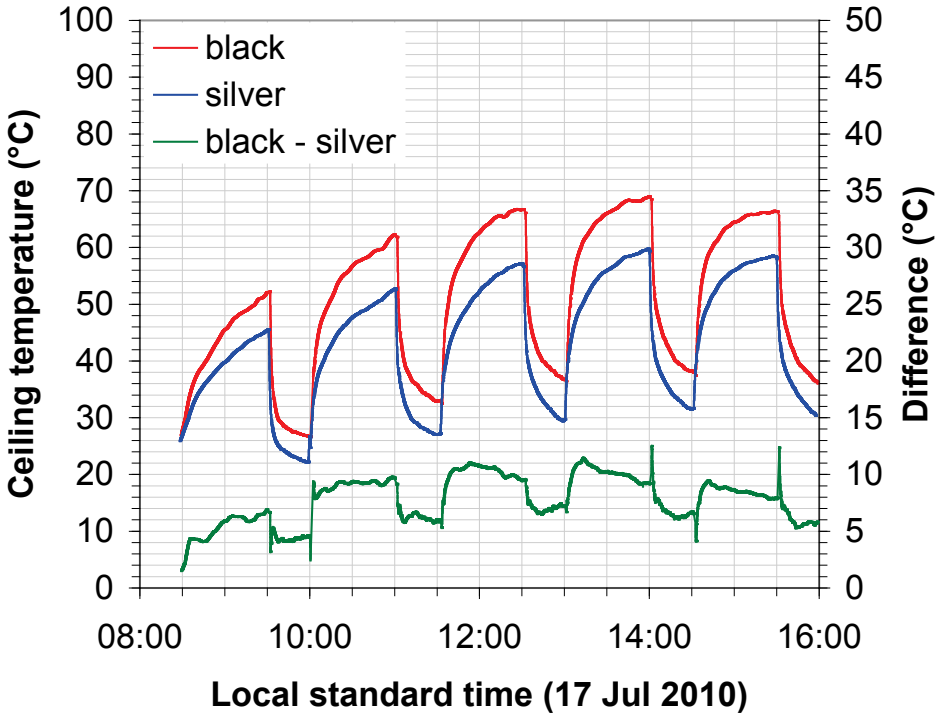
black
silver
black - silver
Ceiling temperature (°C)
Difference (°C)
100
90
80
70
60
50
40
30
20
10
0
50
45
40
35
30
25
20
15
10
5
0
08:00
10:00
12:00
14:00
16:00
Local standard time (17 Jul 2010)

(c)

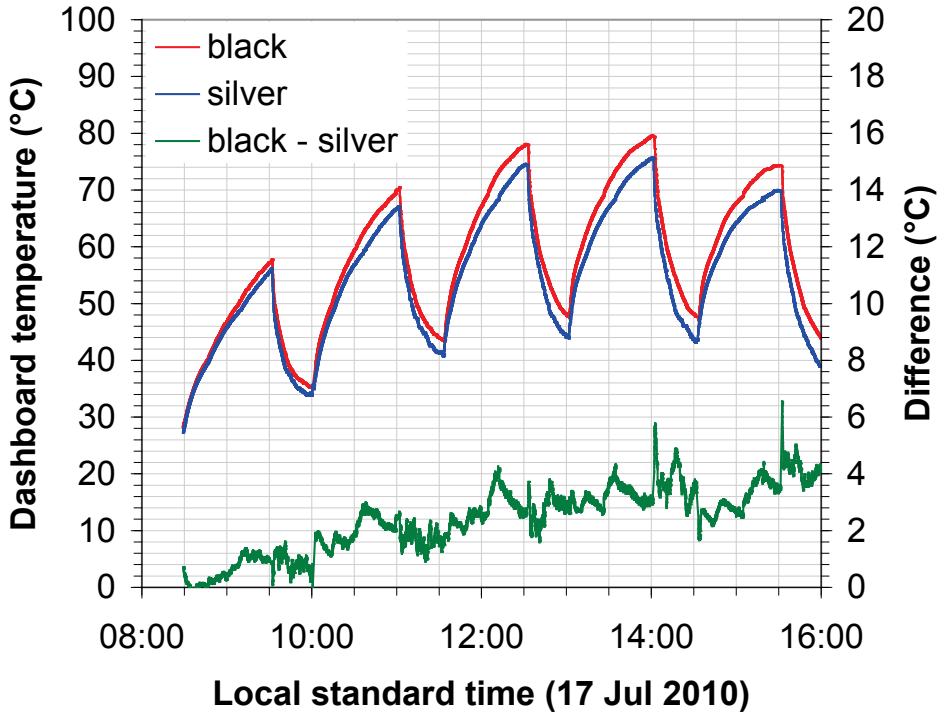
black
silver
black - silver
Dashboard temperature (°C)
Difference (°C)
Local standard time (17 Jul 2010)
08:00
10:00
12:00
14:00
16:00

(d)

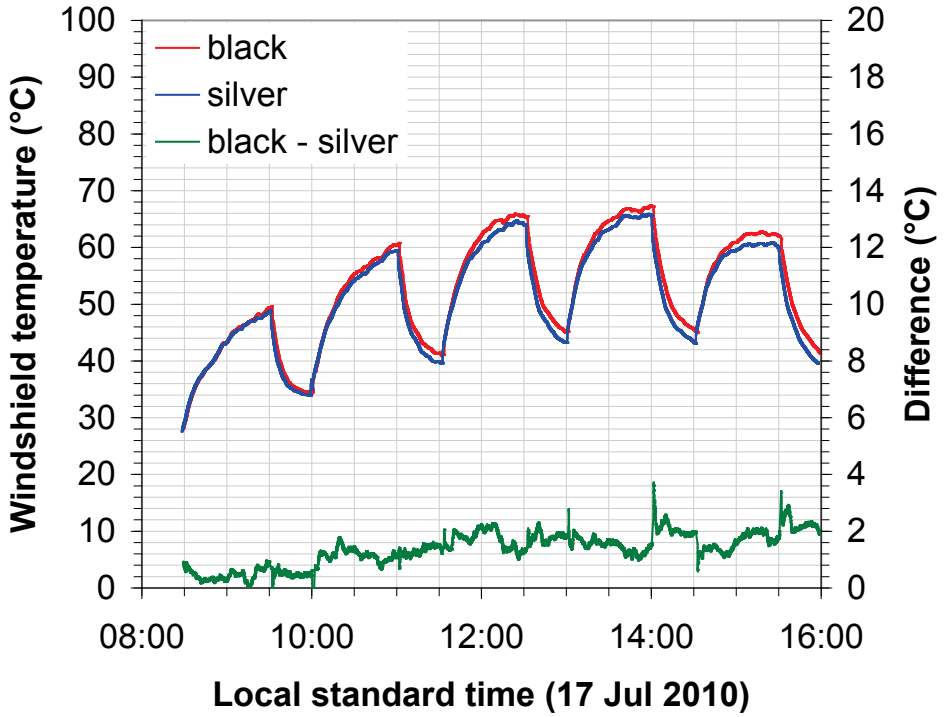
black
silver
black - silver
Windshield temperature (°C)
Difference (°C)
Local standard time (17 Jul 2010)
08:00
10:00
12:00
14:00
16:00

(e)

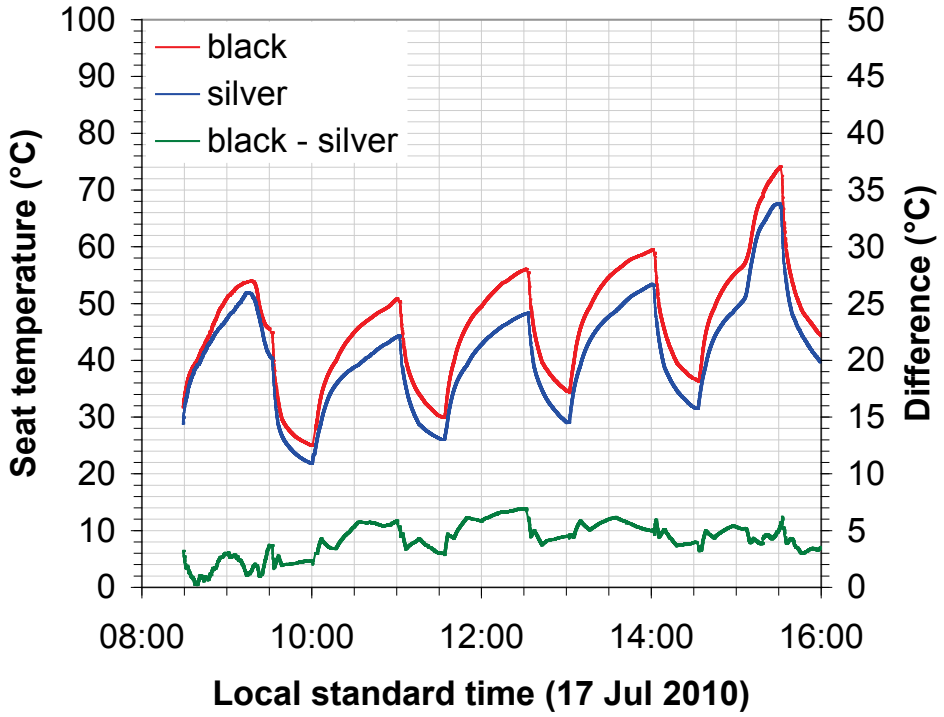
black
silver
black - silver
Seat temperature (°C)
Difference (°C)
Local standard time (17 Jul 2010)
08:00
10:00
12:00
14:00
16:00

(f)

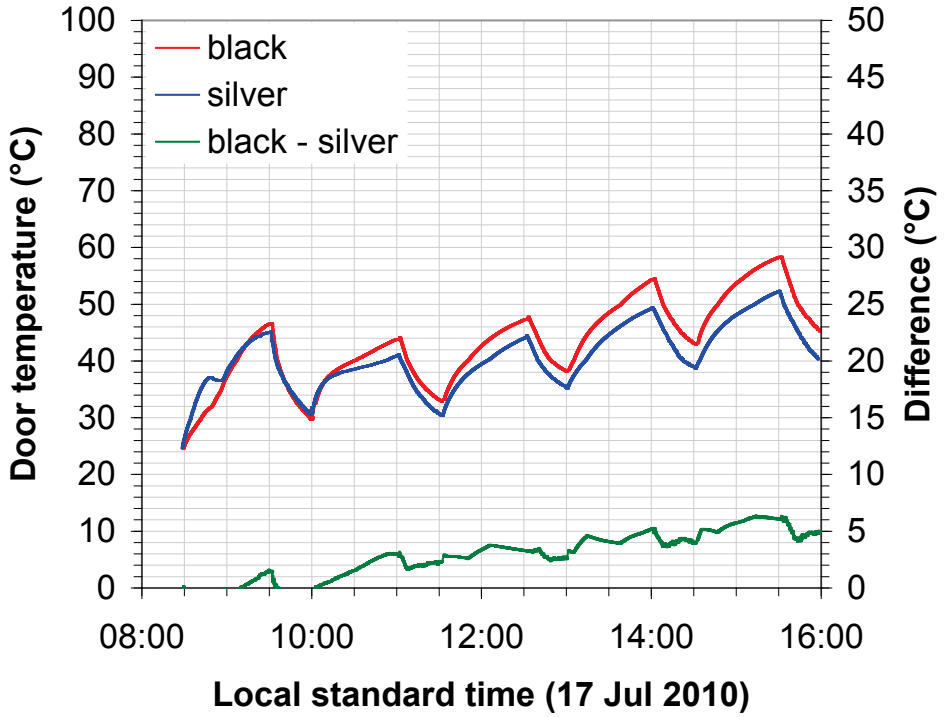
black
silver
black - silver
Door temperature (°C)
Difference (°C)
Local standard time (17 Jul 2010)
08:00
10:00
12:00
14:00
16:00

(g)

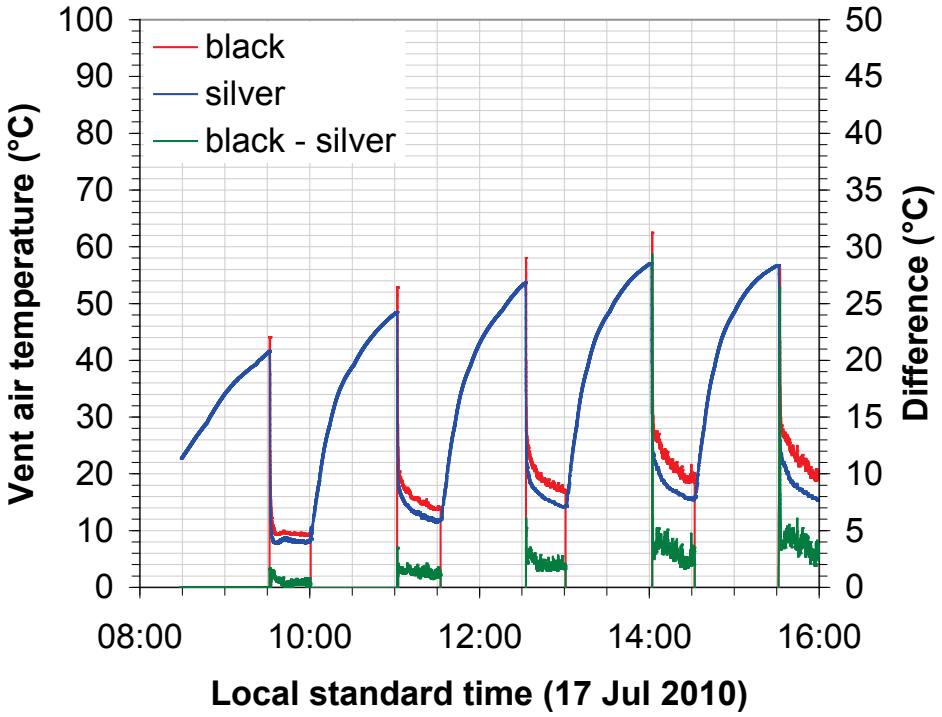

(h)

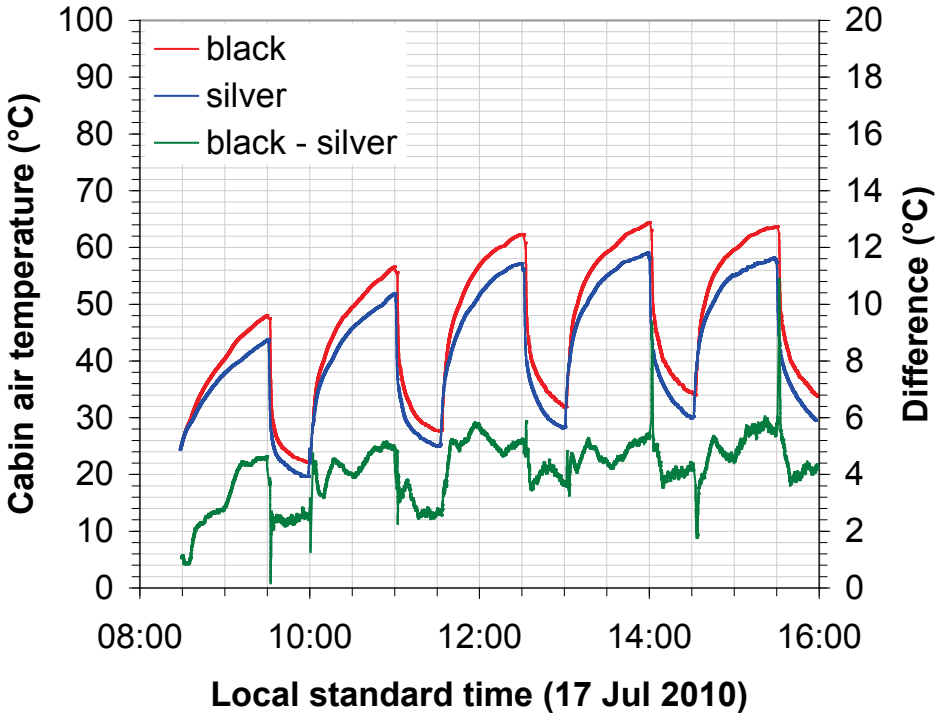

Figure 7. Comparisons of (a) roof, (b) ceiling, (c) dashboard, (d) windshield, (e) seat, (f) door, (g) vent air and (h) cabin air temperatures measured during soaking and cooling trials.

(a)

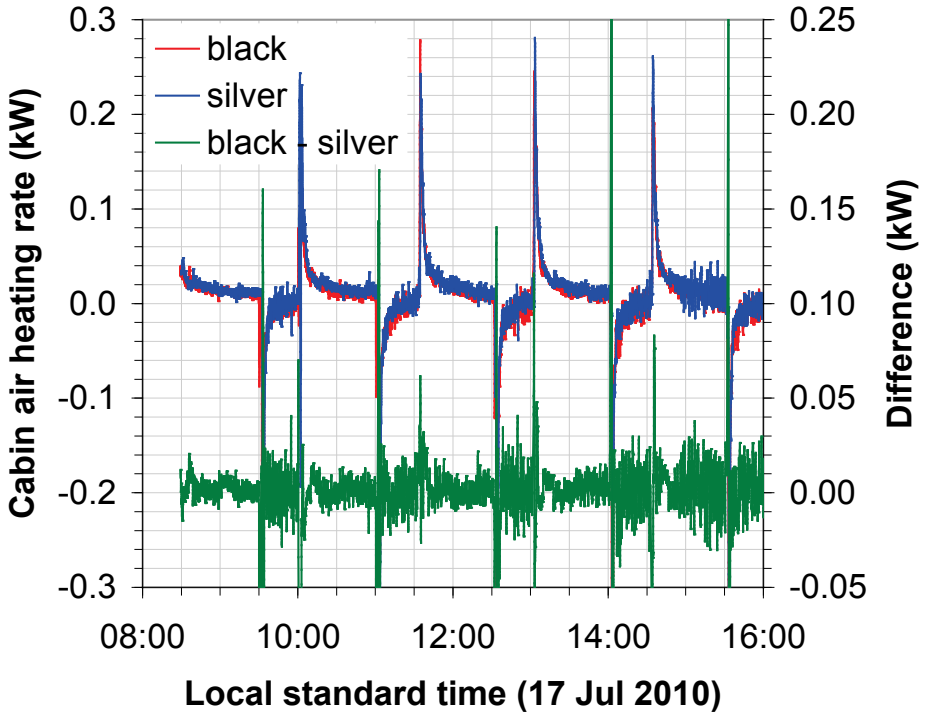

(b)

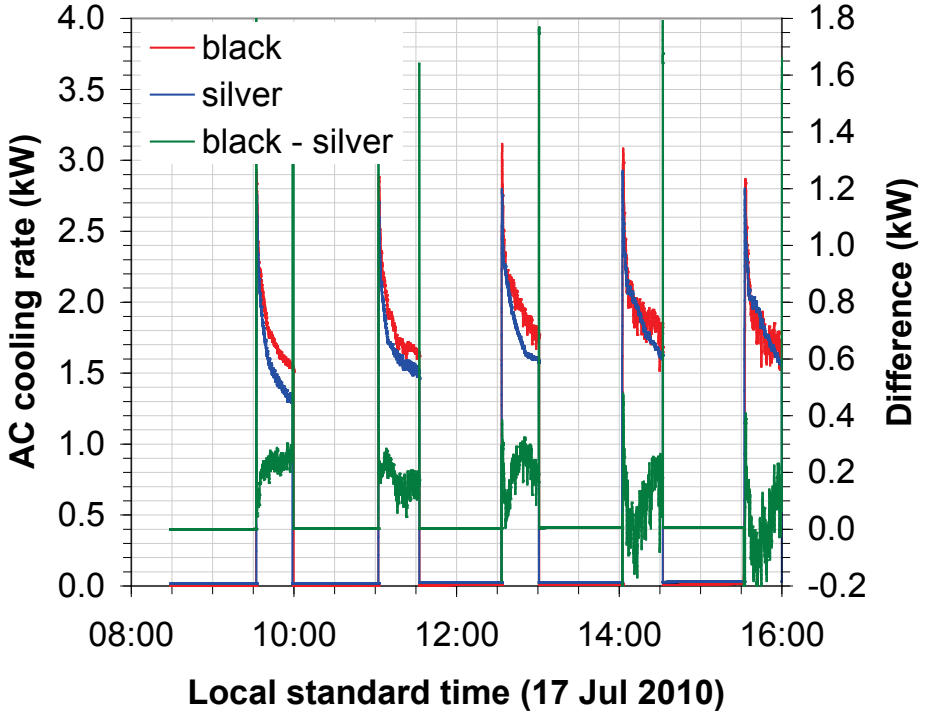

Figure 8. Comparisons of (a) cabin air heating rates measured during soaking and cooling trials and (b) AC cooling rates measured during cooling trials.

(a)

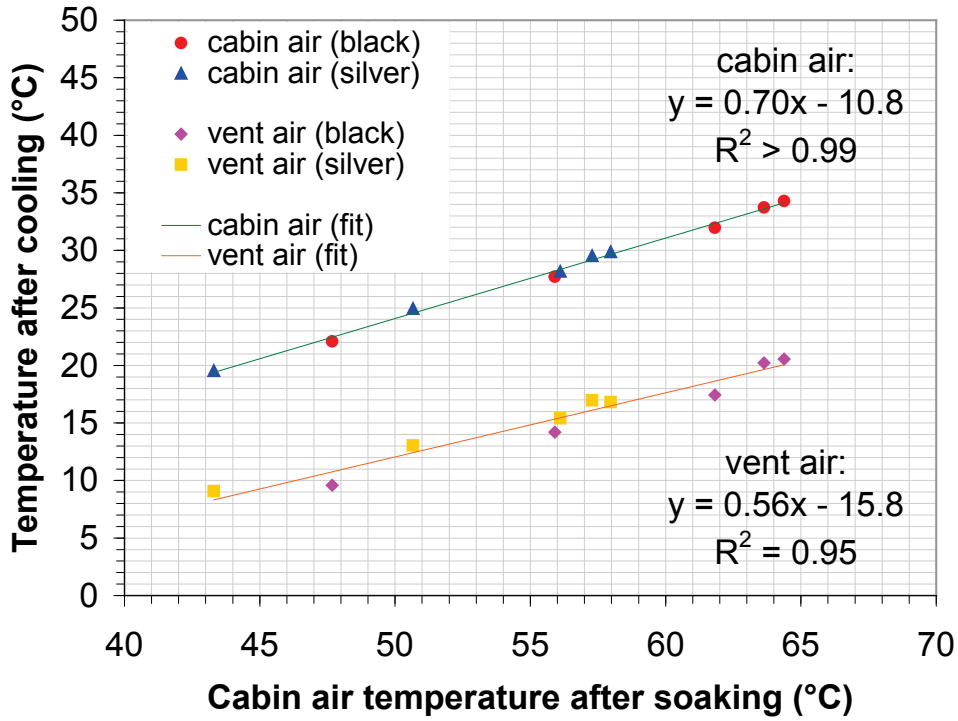

(b)

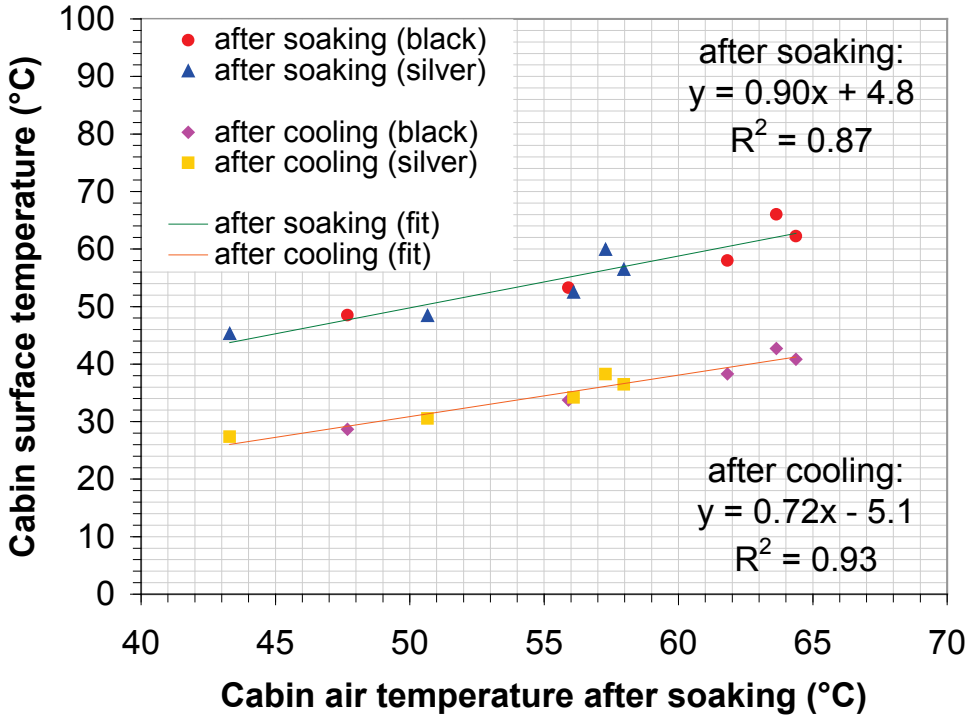

Figure 9. Variations with cabin air final soak temperature of (a) cabin air and vent air final cooldown temperatures and (b) cabin surface final soak and final cooldown temperatures. Soak and cooldown intervals were approximately 60 and 30 min, respectively.

(a)

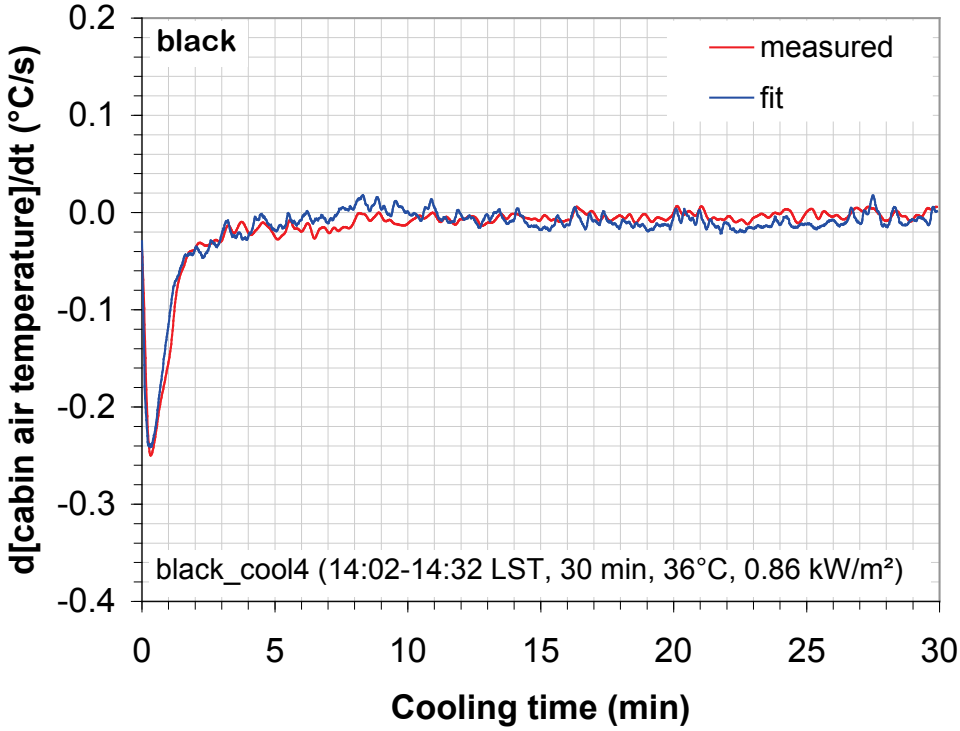

(b)

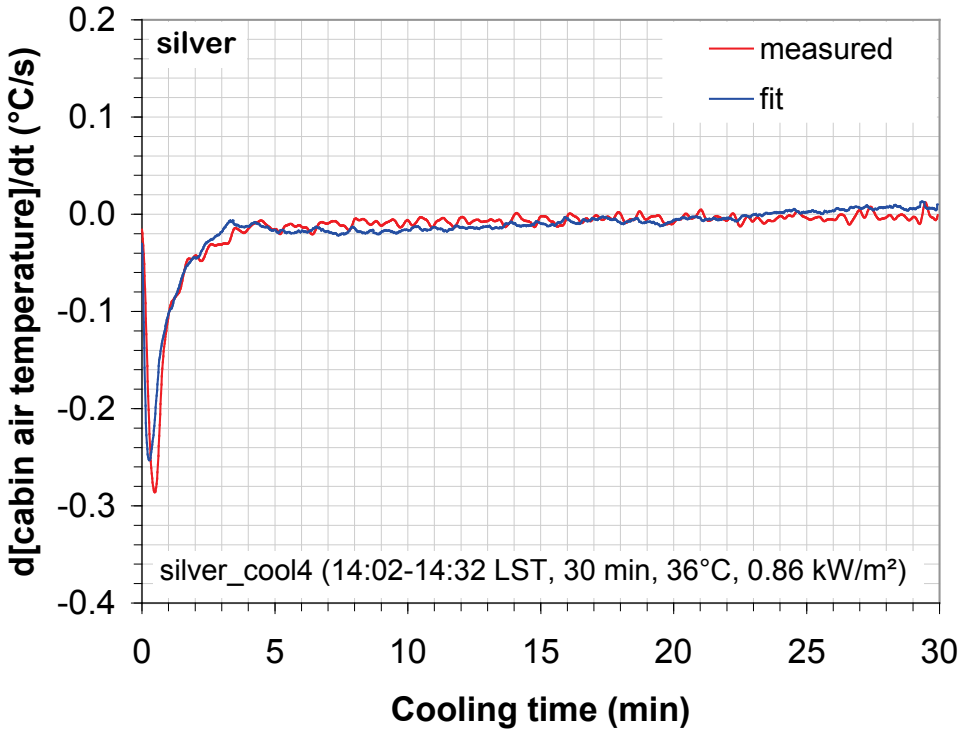

Figure 10. Measured and fitted rates of change of cabin air temperature versus cooling time in Trial 4, shown for (a) the black car and (b) the silver car.

(a)

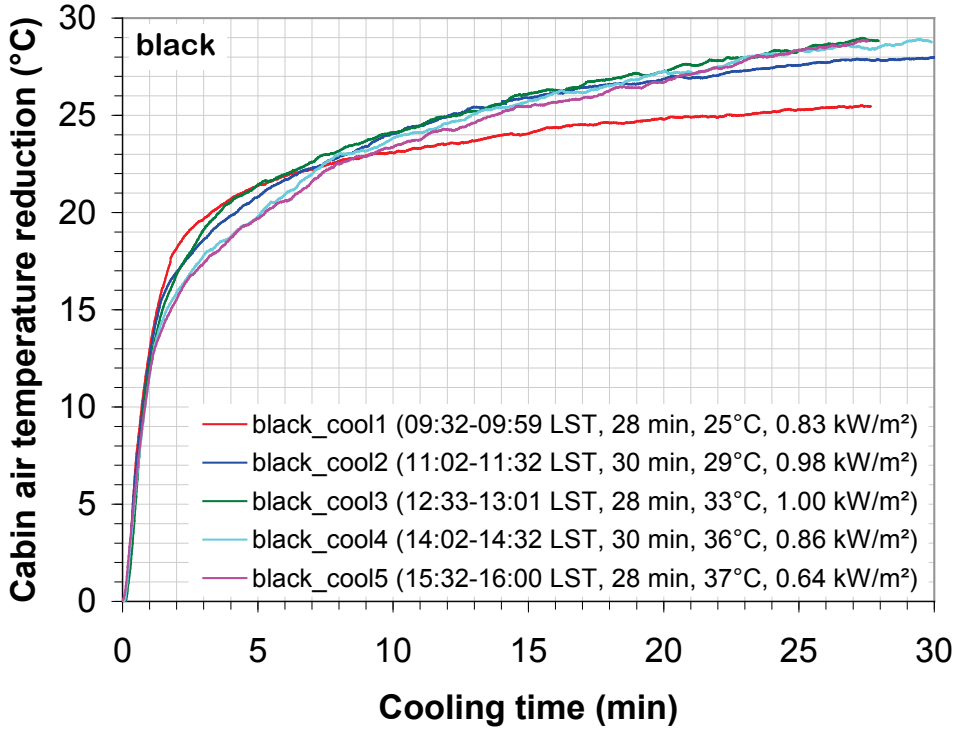

(b)

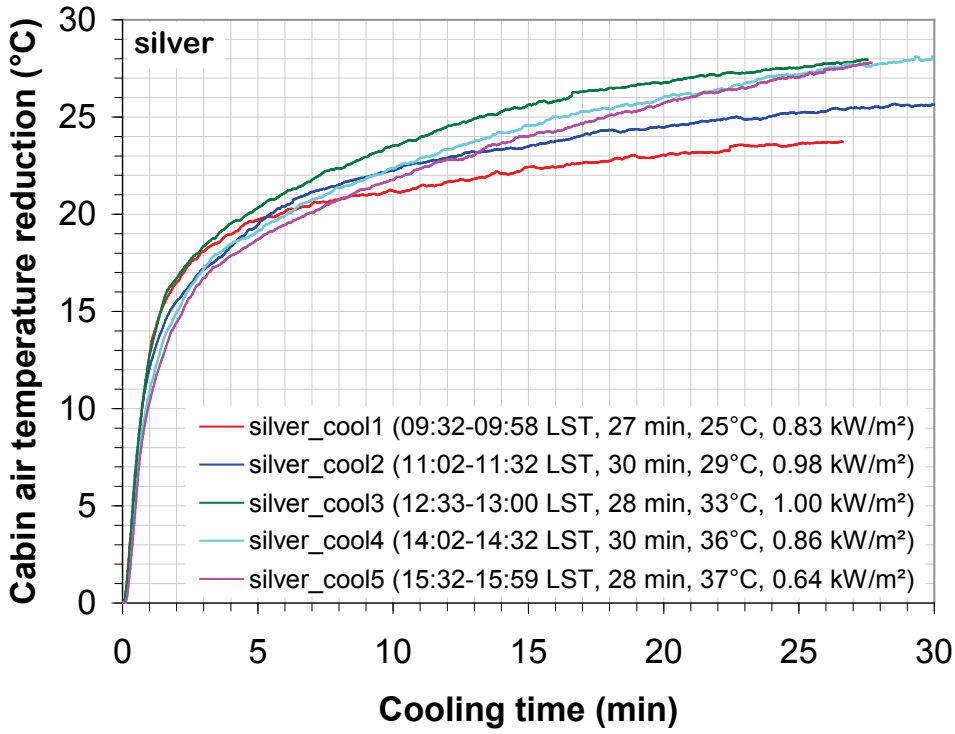

Figure 11. Reduction in cabin air temperature versus cooling time in each of five trials, shown for (a) the black car and (b) the silver car. Cooling trial interval, duration, mean outside air temperature and mean solar irradiance are listed in parentheses.

(a)

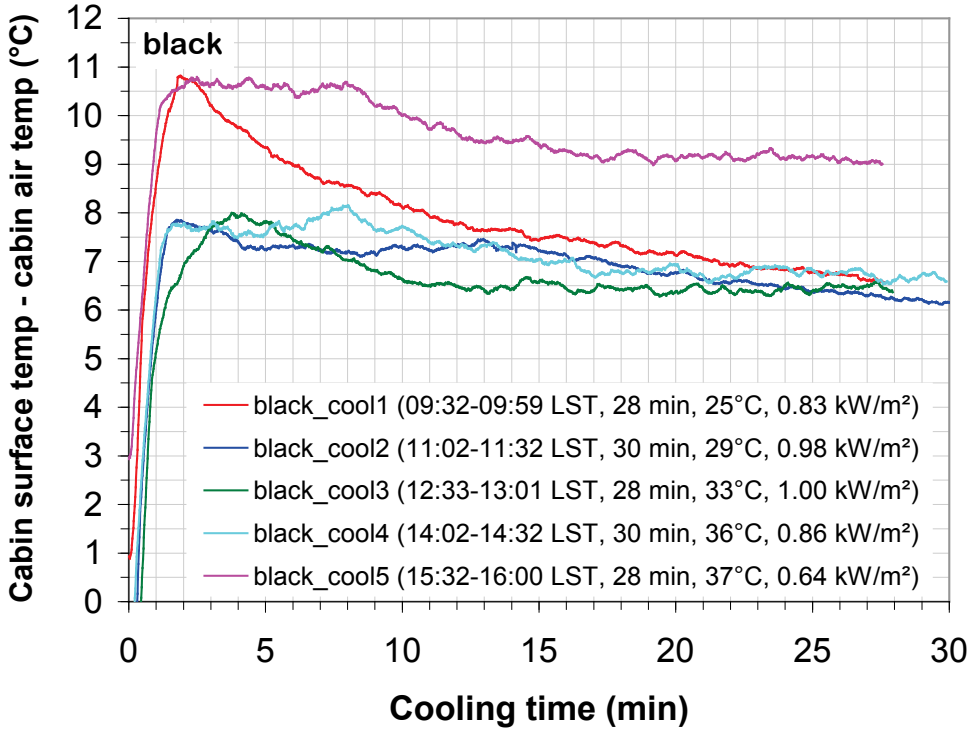

(b)

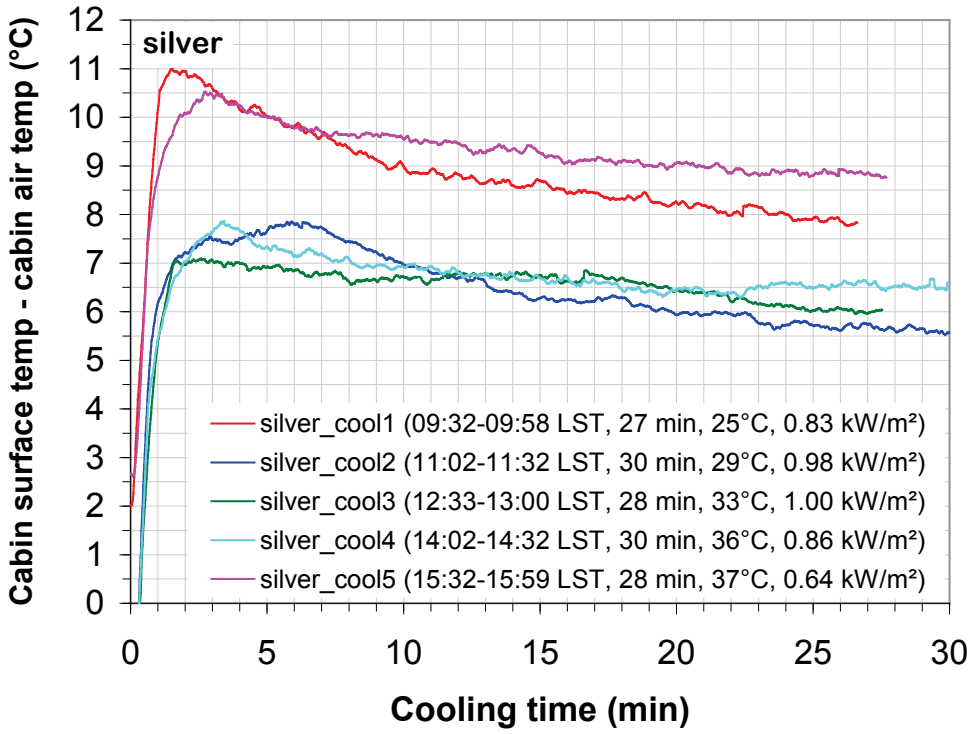

Figure 12. Difference between cabin surface and cabin air temperatures versus cooling time in each of five trials, shown for (a) the black car and (b) the silver car.

(a)

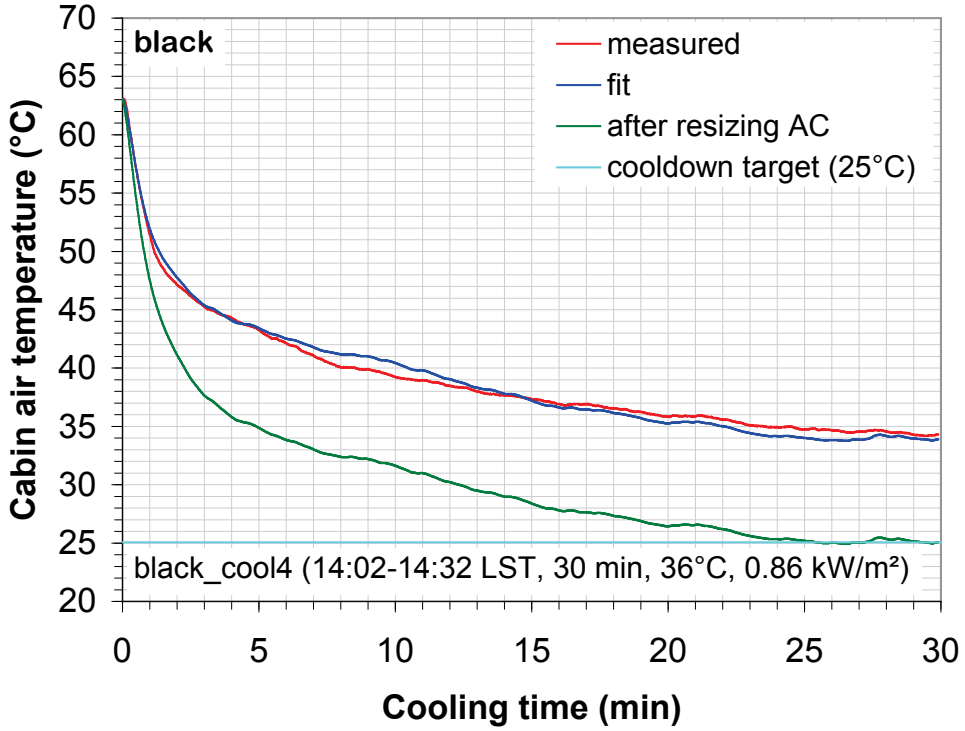

(b)

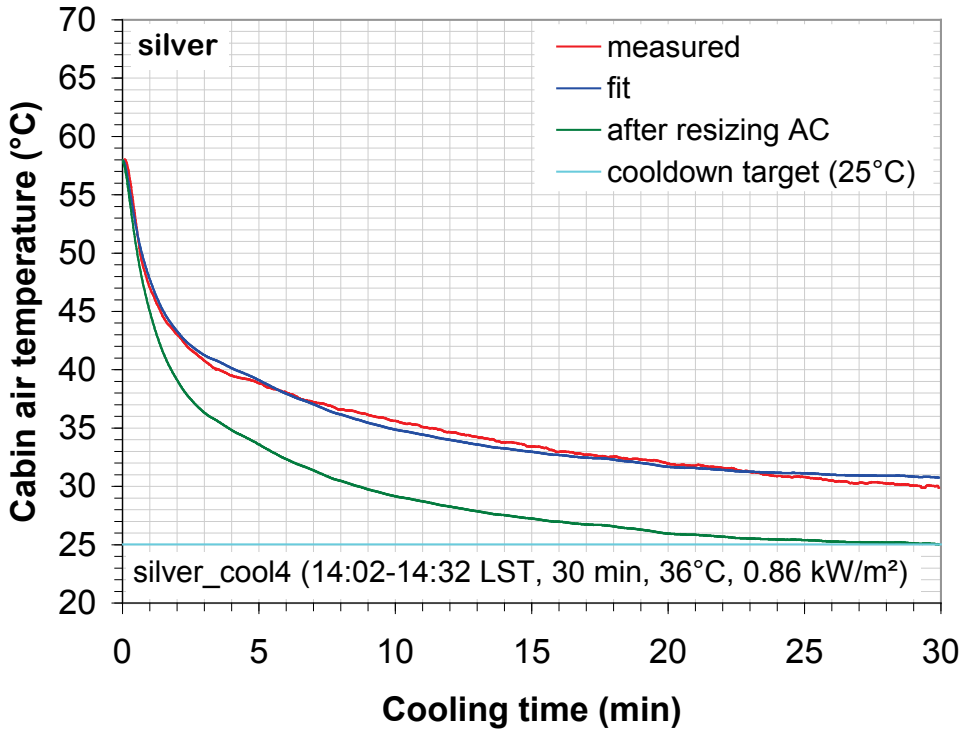

Figure 13. Measured and fitted cabin air temperatures versus cooling time in Trial 4, shown for (a) the black car and (b) the silver car. Each graph also shows the cabin air temperature time series predicted after the AC is resized to attain a target final cabin air temperature of 25°C.

(a)

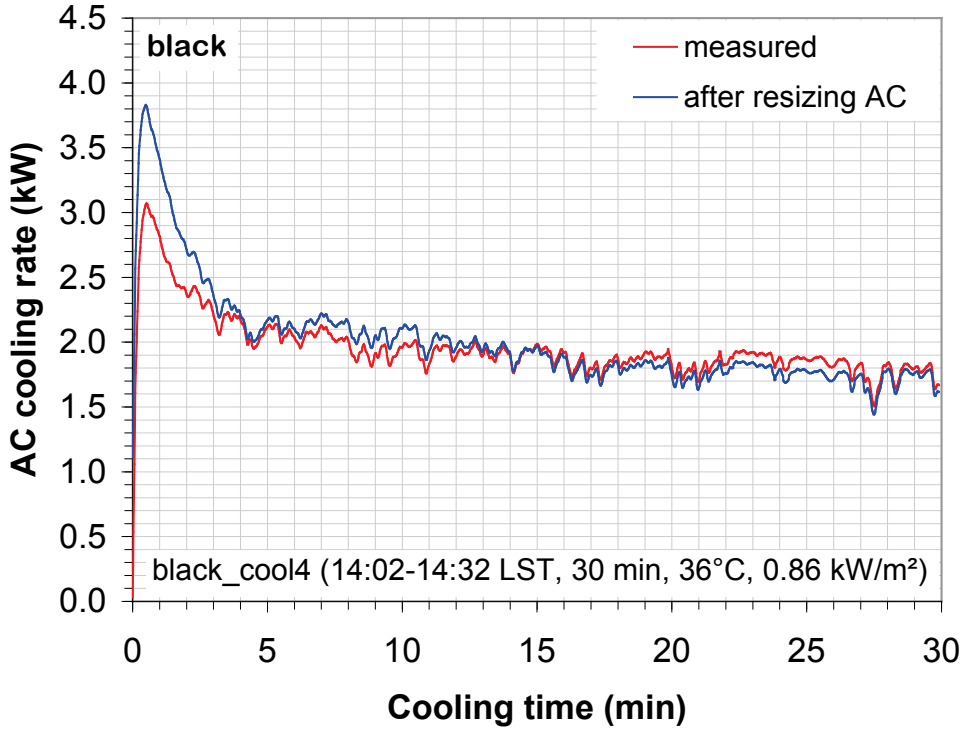

(b)

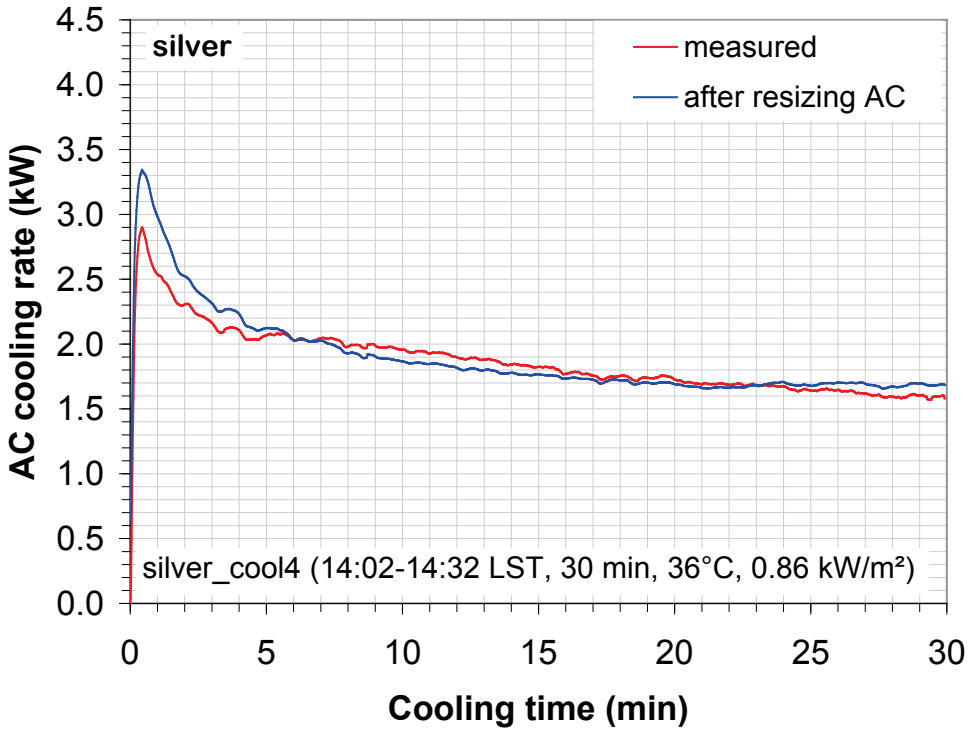

Figure 14. Measured AC cooling rate in Trial 4 shown for (a) the black car and (b) the silver car. Each graph also shows the cooling rate predicted after the AC is resized to attain a target final cabin air temperature of 25°C.

(a)

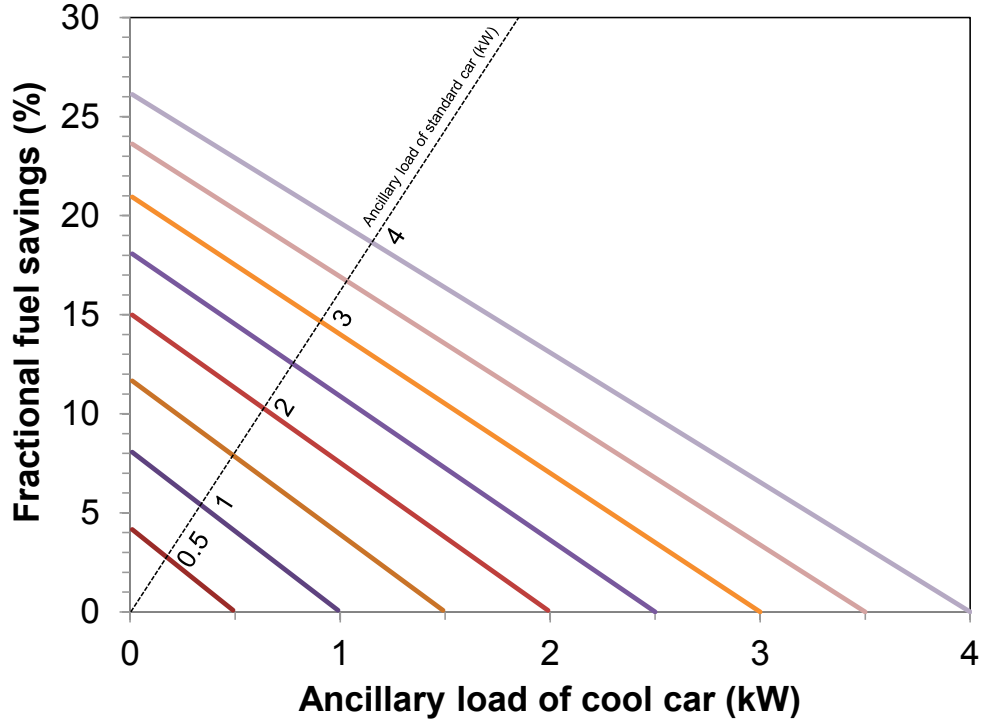
Fractional fuel savings (%)
Ancillary load of cool car (kW)
Ancillary load of standard car (kW)
0.5
1
2
3
4
0
5
10
15
20
25
30
0
1
2
3
4

(b)

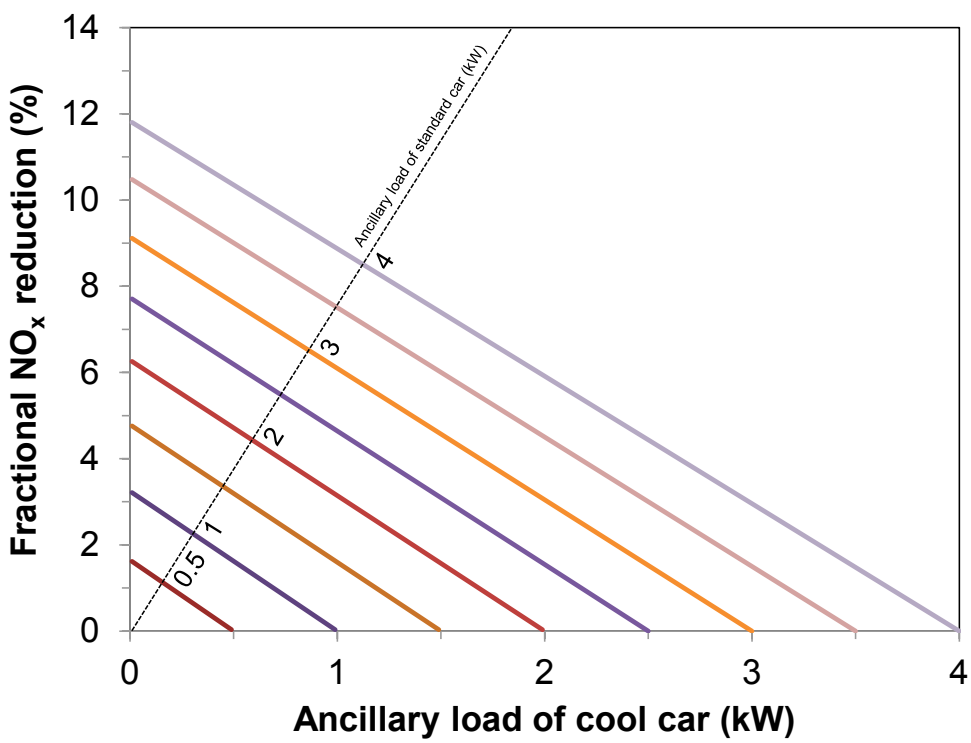
Fractional NOx reduction (%)
Ancillary load of cool car (kW)
Ancillary load of standard car (kW)
0.5
1
2
3
4
0
2
4
6
8
10
12
14
0
1
2
3
4

(c)

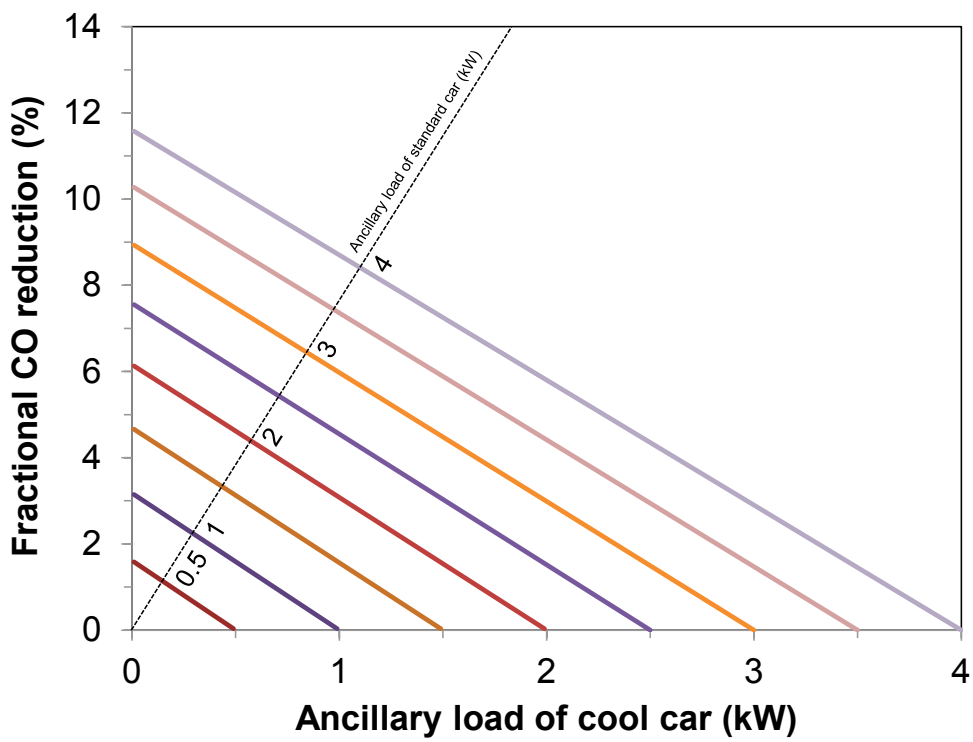

(d)

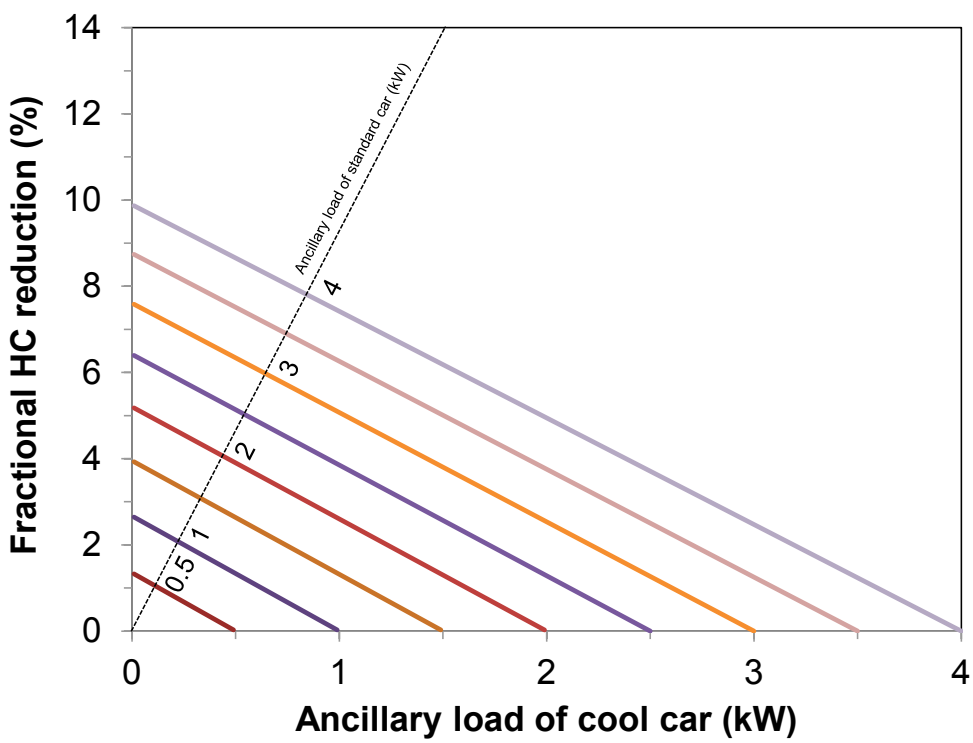

Figure 15. Fractional reductions in rates of (a) fuel consumption, (b) NO_x emission, (c) CO emission and (d) HC emission as a function of ancillary loads of the standard (black) and cool (nonblack) cars for the SC03 driving cycle. Each curve represents a different value for ancillary load of the standard car. Results represent a vehicle with a power rating of 84 kW.

(a)

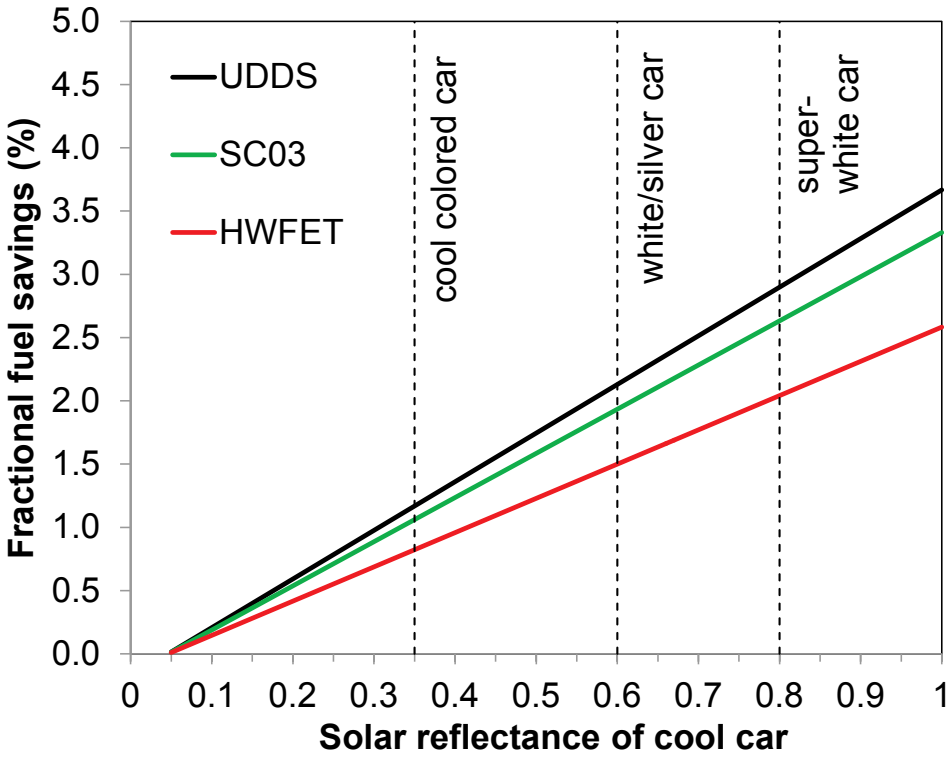
5.0
4.5
4.0
3.5
3.0
2.5
2.0
1.5
1.0
0.5
0.0
Fractional fuel savings (%)
UDDS
SC03
HWFET
cool colored car
white/silver car
super-
white car
0
0.1
0.2
0.3
0.4
0.5
0.6
0.7
0.8
0.9
1
Solar reflectance of cool car

(b)

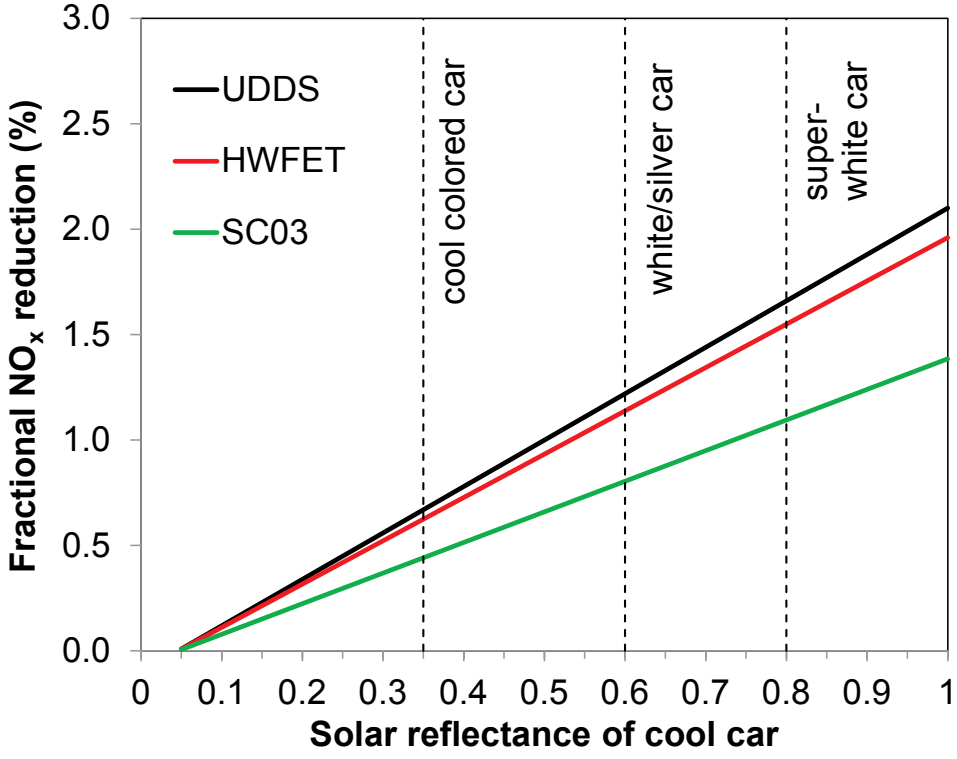
3.0
2.5
2.0
1.5
1.0
0.5
0.0
Fractional NOx reduction (%)
UDDS
HWFET
SC03
cool colored car
white/silver car
super-
white car
0
0.1
0.2
0.3
0.4
0.5
0.6
0.7
0.8
0.9
1
Solar reflectance of cool car

(c)

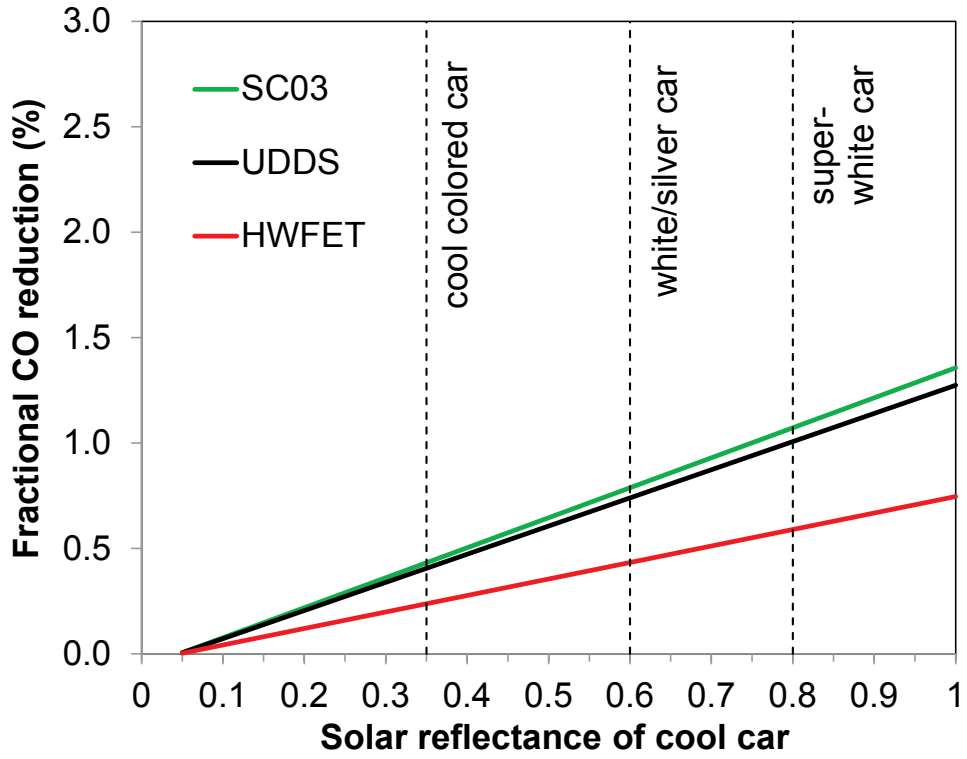

(d)

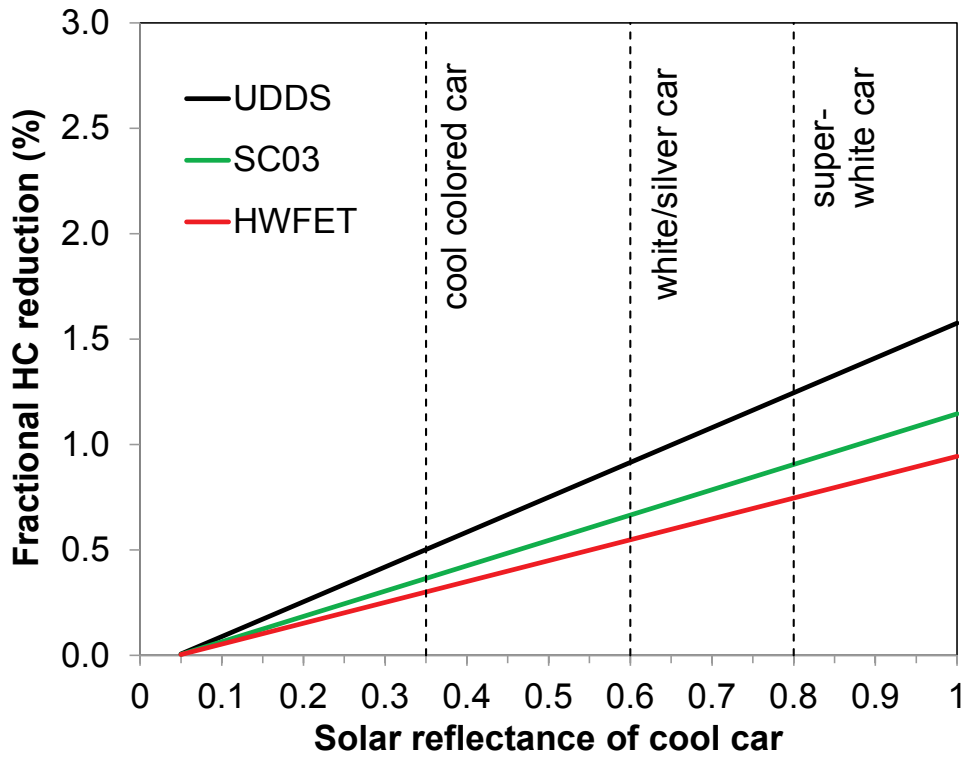

Figure 16. Fractional reductions in rates of (a) fuel consumption, (b) NO_x emission, (c) CO emission and (d) HC emission versus solar reflectance of the cool car shell, assuming a vehicle power rating of 84 kW. Reference values of solar reflectance for a typical cool colored car, a typical white or silver car, and a hypothetical super-white car are shown as dashed vertical lines.

(a)

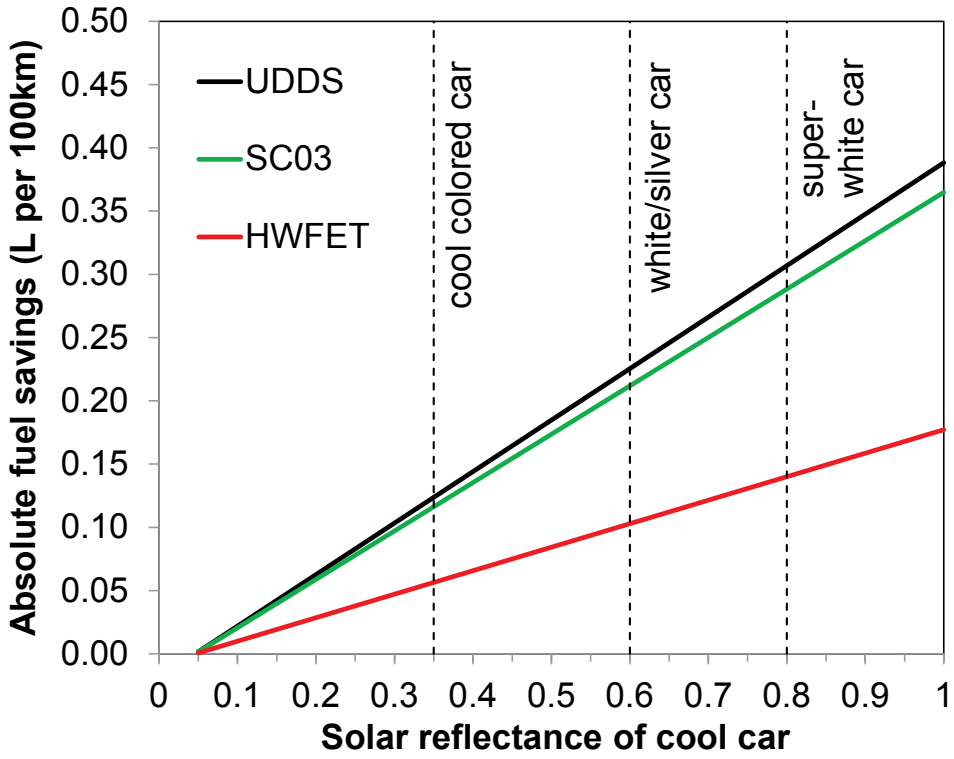
Absolute fuel savings (L per 100km)
0.50
0.45
0.40
0.35
0.30
0.25
0.20
0.15
0.10
0.05
0.00
UDDS
SC03
HWFET
cool colored car
white/silver car
super-
white car
0
0.1
0.2
0.3
0.4
0.5
0.6
0.7
0.8
0.9
1
Solar reflectance of cool car

(b)

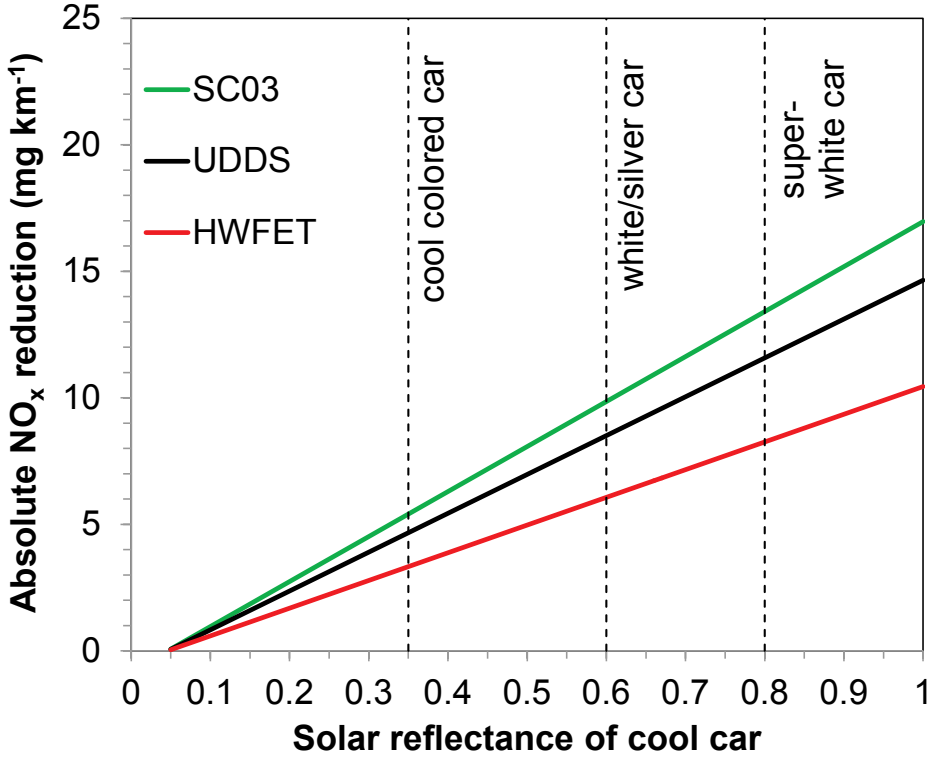
Absolute NOx reduction (mg km-1)
25
20
15
10
5
0
SC03
UDDS
HWFET
cool colored car
white/silver car
super-
white car
0
0.1
0.2
0.3
0.4
0.5
0.6
0.7
0.8
0.9
1
Solar reflectance of cool car

(c)

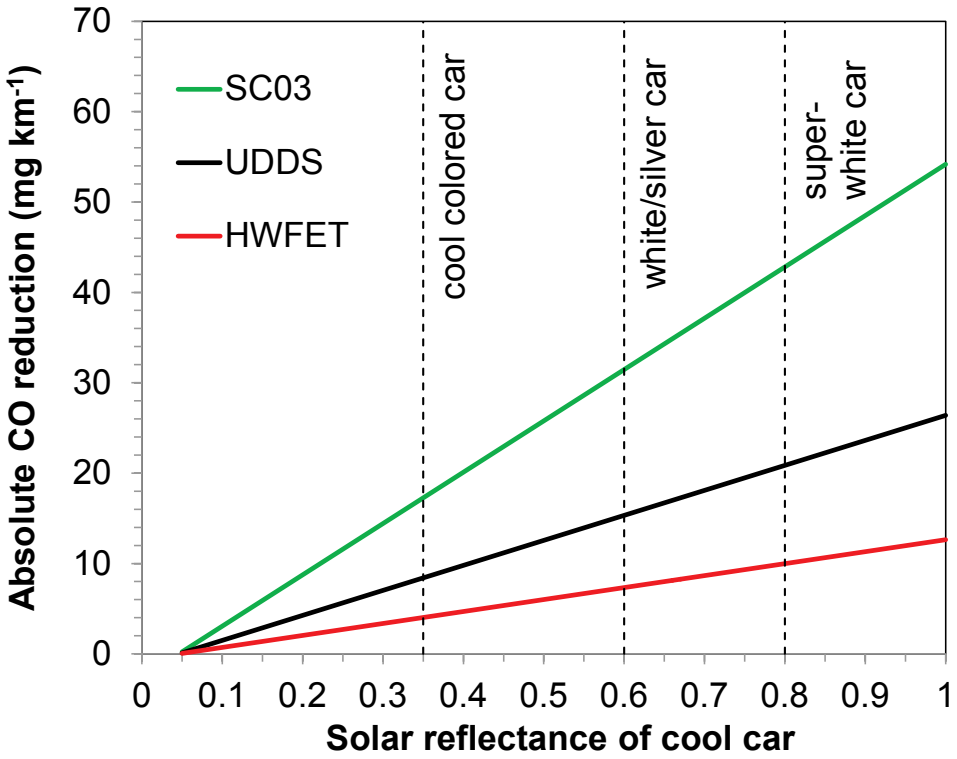

(d)

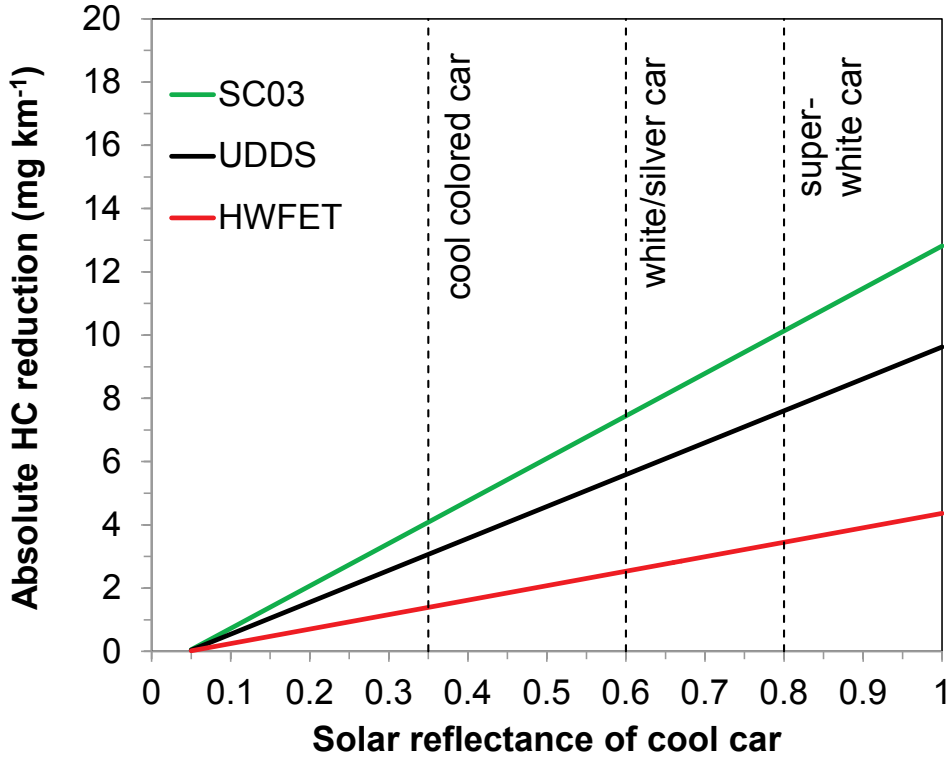

Figure 17. Absolute reductions in rates of (a) fuel consumption, (b) NO_x emission, (c) CO emission and (d) HC emission versus solar reflectance of the cool car shell. Reference values of solar reflectance for a typical cool colored car, a typical white or silver car, and a hypothetical super-white car are shown as dashed vertical lines.